A novel monomeric amyloid β-activated signaling pathway regulates brain development via inhibition of microglia

Hyo Jun Kwon, Devi Santhosh, and Zhen Huang*

Departments of Neurology and Neuroscience

University of Wisconsin-Madison

Madison, WI 53706, USA

* Author for correspondence

Tel.: 608-263-2469

Email: zhuang3@wisc.edu

Running title: Monomeric Aβ pathway inhibits microglia in developing brain

19

20

ABSTRACT

Amyloid β (Aβ) forms aggregates in the Alzheimer's disease brain and is well known for its pathological roles. Recent studies show that it also regulates neuronal physiology in the healthy brain. Whether Aβ also regulates glial physiology in the normal brain, however, has remained unclear. In this article, we describe the discovery of a novel signaling pathway activated by the monomeric form of Aβ that plays essential roles in the regulation of microglial activity and the assembly of neocortex during development. We find that activation of this pathway depends on the function of amyloid precursor (APP) and heterotrimeric G proteins in microglia and inhibits microglial immune activation at transcriptional and post-transcriptional levels. Genetic disruption of this pathway during neocortical development results in microglial dysregulation and excessive matrix proteinase activation, leading to basement membrane degradation, neuronal ectopia, and laminar disruption. These results uncover a previously unknown function of Aβ as a negative regulator of brain microglia and substantially elucidate the molecular mechanisms underlying this regulation. Considering the prominence of Aβ and neuroinflammation in the pathology of Alzheimer's disease, they also highlight a potentially overlooked role of Aβ monomer depletion in the development of the disease.

INTRODUCTION

43 Aβ, a core component of amyloid plaques in the Alzheimer's disease brain, is well known to form
44 oligomers under disease conditions. Studies have shown that the oligomers formed by Aβ are highly
45 toxic, with wide-ranging effects including inhibition of neurotransmitter release, depletion of synaptic
46 vesicle pools, disruption of postsynaptic organization and function, and impairment of multiple forms of
47 synaptic plasticity (Gulisano et al., 2018; He et al., 2019; Kim et al., 2013; Lauren et al., 2009; Lazarevic et
48 al., 2017; Parodi et al., 2010; Puzzo et al., 2008; Shankar et al., 2008; Walsh et al., 2002; Yang et al.,
49 2015; Zott et al., 2019). These effects likely significantly underpin the pathogenic role of Aβ in
50 Alzheimer's disease and contribute to neuron loss and cognitive decline in patients. Besides its
51 pathological roles, recent studies show that Aβ is also produced in the healthy brain by neurons in a
52 neural activity-dependent manner and regulates the normal physiology of neurons (Cirrito et al., 2005;
53 Fogel et al., 2014; Galanis et al., 2021; Garcia-Osta and Alberini, 2009; Gulisano et al., 2018; Gulisano et
54 al., 2019; Morley et al., 2010; Palmeri et al., 2017; Puzzo et al., 2008; Zhou et al., 2022). For example,
55 consistent with studies showing that Aβ monomers and low molecular weight oligomers positively
56 regulate synaptic function and plasticity, administration of these molecules in vivo has been found to
57 improve learning and memory in animals (Fogel et al., 2014; Garcia-Osta and Alberini, 2009; Gulisano et
58 al., 2018; Gulisano et al., 2019; Morley et al., 2010; Palmeri et al., 2017; Puzzo et al., 2008). Recent
59 studies have further shown that Aβ monomers directly promote synapse formation and function and
60 homeostatic plasticity, processes crucial to normal cognitive function (Galanis et al., 2021; Kamenetz et
61 al., 2003; Zhou et al., 2022). Together, these findings have provided crucial insights into the
62 physiological roles that Aβ plays in regulating normal neuronal function in the brain. However, it
63 remains unclear if Aβ also regulates the physiology of glia, nonneuronal cells that also play important
64 roles in normal brain function.
65

66 Microglia and astrocytes, two of the major glial cell types in the brain, are known to play critical
67 roles in the normal development, function, and plasticity of the brain circuitry (Barres, 2008; Schafer and
68 Stevens, 2015). They coordinately regulate, among others, the spatiotemporally specific expression of
69 immune cytokines in the brain that regulate numerous processes in brain circuit development, function,
70 and plasticity (Zipp et al., 2023). For example, in the thalamus, a key relay station in the visual pathway,
71 populations of astrocytes have been found to activate the expression of interleukin-33 in a neural
72 activity-dependent manner, induce activity-dependent elimination of supernumerary synapses, and
73 promote the maturation of the visual circuitry in early postnatal life (Vainchtein et al., 2018). In the
74 adult hippocampus, in contrast, astrocytes have been found to activate the expression of interleukin-33
75 under neuronal activity blockade and induce homeostatic synaptic plasticity that maintains circuit
76 activity balance (Wang et al., 2021). In the striatum and the neocortex, not only have astrocytes but
77 also have microglia been observed to activate the expression of TNFα upon changes in neural circuit
78 activity and induce homeostatic synaptic plasticity that dampens circuit perturbation (Heir et al., 2024;
79 Lewitus et al., 2016; Stellwagen and Malenka, 2006). In the clinic, the induction of microglial release of
80 cytokines such as TNFα also underpins the application of repetitive transcranial magnetic stimulation, a
81 noninvasive brain stimulation technique frequently used to induce cortical plasticity and treat
82 pharmaco-resistant depression (Eichler et al., 2023). Furthermore, in neurodegenerative diseases such
83 as Alzheimer's disease, glial activation and brain cytokine elevation are key pathologic factors in disease
84 development (Colonna and Butovsky, 2017; Patani et al., 2023). Elevated TNFα expression by microglia
85 also underlies interneuron deficits and autism-like phenotype linked to maternal immune activation (Yu
86 et al., 2022). Thus, the precise regulation of glial cytokine expression in the brain plays a key role in the
87 normal development and function of the brain and its dysregulation is linked to common
88 neurodevelopmental and neurodegenerative diseases. However, how glial cytokine expression is
89 mechanistically regulated by cell-cell communication in the brain have remained largely unknown.

90

91 In this article, we report the discovery of a novel microglial signaling pathway activated by Aβ,
92 the neuron-produced peptide at the center of Alzheimer's disease, that plays a crucial role in precisely
93 regulating the levels of microglial cytokine expression and activity and ensuring the proper assembly of
94 neuronal laminae during cerebral cortex development. We first came across this pathway in our study
95 of the function of *ric8*a, a gene encoding a molecular chaperone for heterotrimeric G proteins (Gabay et
96 al., 2011; Ma et al., 2012; Ma et al., 2017; Tall et al., 2003). We found that deletion of *ric8a* during
97 cortical development resulted in cortical basement membrane degradation, neuronal ectopia, and
98 laminar disruption. However, unlike in classic models of cobblestone lissencephaly, these phenotypes
99 resulted not from *ric8a* deficiency in brain neural cell types, but from deficiency in microglia. The
100 phenotypes also resemble those in mutants of amyloid precursor protein (APP) family and pathway
101 genes. Indeed, we found that *app* deficiency in microglia also underpins ectopia formation in *app* family
102 gene mutants. Furthermore, we found that APP and Ric8a form a functional pathway in microglia that is
103 specifically activated by the monomeric form of Aβ and this pathway normally inhibits the
104 transcriptional and post-transcriptional expression of immune cytokines by microglia.

105 **RESULTS**

106 **Cortical ectopia in *ric8a-emx1-cre* mutants results from non-neural deficiency**

107 To study of the function of *ric8a* in neocortical development, we deleted a conditional *ric8a* allele (Ma et
108 al., 2012; Ma et al., 2017) using *emx1-cre,* a *cre* line designed to target dorsal forebrain neural
109 progenitors in mice (Gorski et al., 2002). We found it result in ectopia formation exclusively in the lateral
110 cortex of the perinatal mutant brain (**Fig. 1a-d**). Birth-dating showed that the ectopia consisted of both
111 early and late-born neurons (**Supplemental Fig. 1**). Consistent with this observation, neurons in the
112 ectopia also stained positive for both Ctip2 and Cux1, genes specific to lower and upper-layer neurons,
113 respectively. Interestingly, in cortical areas without ectopia, radial migration of early- and late-born
114 neurons appeared largely normal as shown by birth-dating as well as Cux1 and Ctip2 staining
115 (**Supplemental Fig. 2**). This suggests that cell-autonomous defects in neurons are unlikely the cause of
116 the ectopia. At E16.5, clear breaches in the pial basement membrane of the developing cortex were
117 already apparent (**Supplemental Fig. 3**). However, unlike classic models of cobblestone lissencephaly,
118 where radial glial fibers typically retract, radial glial fibers in *ric8a* mutants instead extended beyond the
119 breaches. This argues against radial glial cell adhesion defects since they would be predicted to retract.
120 Furthermore, in areas without ectopia, we also observed normal localization of Cajal-Retzius cells,
121 expression of Reelin, and splitting of the preplate, arguing against primary defects in Cajal-Retzius cells.
122 In cobblestone lissencephaly, studies show that ectopia result from primary defects in radial glial
123 maintenance of the pial basement membrane (Beggs et al., 2003; Graus-Porta et al., 2001; Moore et al.,
124 2002; Satz et al., 2010). In *ric8a* mutants, we observed large numbers of basement membrane breaches
125 at E14.5, almost all associated with ectopia (**Supplemental Fig. 4**). In contrast, at E13.5, although we
126 also observed significant numbers of breaches, none was associated with ectopia. This indicates that
127 basement membrane breaches similarly precede ectopia in *ric8a* mutants. However, at E12.5, despite a
128 complete lack of basement membrane breaches, we observed increased numbers of laminin-positive

129 debris across the lateral cortex, both beneath basement membrane segments with intact laminin
130 staining and beneath segments with disrupted laminin staining, the latter presumably sites of future
131 breach (**Supplemental Fig. 5**). As a major basement membrane component, the increased amounts of
132 laminin debris suggest increased degradative activity within the developing cortex. Thus, these results
133 indicate that excessive basement membrane degradation, but not defective maintenance, is likely a
134 primary cause of cortical ectopia in *ric8a* mutants.

135

136 To determine the cell type(s) genetically responsible for cortical basement membrane
137 degradation and ectopia in *ric8a* mutants, we employed a panel of *cre* lines (**Fig. 1e-h'**). To target Cajal-
138 Retzius cells, we employed *wnt3a-cre* (Yoshida et al., 2006) but found *ric8a* deletion using *wnt3a-cre* did
139 not result in ectopia. To target postmitotic excitatory and inhibitory neurons, we employed *nex-cre*
140 (Goebbels et al., 2006) and *dlx5/6-cre* (Stenman et al., 2003) respectively but similarly found neither
141 result in ectopia. These results point to *ric8a* requirement in cell types other than post-mitotic neurons.
142 To test the involvement of neural progenitors, we employed *nestin-cre* (Graus-Porta et al., 2001).
143 Previous studies show that deletion of *β1 integrin* and related genes by *emx1-cre* and *nestin-cre* results
144 in similar ectopia phenotypes (Belvindrah et al., 2006; Graus-Porta et al., 2001; Huang et al., 2006;
145 Niewmierzycka et al., 2005). To our surprise, deletion of *ric8a* by *nestin-cre* did not result in ectopia (Ma
146 et al., 2017) (**Fig. 1g-g'**). Since *nestin-cre*-mediated deletion in neural progenitors is inherited by post-
147 mitotic neurons and astrocytes, this indicates that the combined deletion of *ric8a* from all these cell
148 types does not lead to ectopia. The onset of *nestin-cre* expression is, however, developmentally slightly
149 later than that of *emx1-cre* (Gorski et al., 2002). To assess the potential contribution of this temporal
150 difference, we employed *foxg1-cre*, a *cre* line expressed in forebrain neural progenitors starting from
151 E10.5 (Hebert and McConnell, 2000). We found that *ric8a* deletion using *foxg1-cre* still failed to produce

152 ectopia (**Fig. 1h-h'**). Thus, these results strongly argue against the interpretation that *ric8a* deficiency in
153 neural cell lineages is responsible for basement membrane degradation and ectopia in *ric8a* mutants.

154

155 During embryogenesis, the neural tube undergoes epithelial-mesenchymal transition giving rise
156 to neural crest cells (Leathers and Rogers, 2022). This process involves region-specific basement
157 membrane breakdown that resembles the *ric8a* mutant phenotype. To determine if ectopic epithelial-
158 mesenchymal transition plays a role, we examined potential changes in neuro-epithelial cell fates in the
159 mutant cortex. We found that cortical neural progenitors expressed Pax6, Nestin, and Vimentin
160 normally (**Supplemental Fig. 6**). Cell proliferation in the ventricular zone was also normal. Furthermore,
161 although *ric8a* regulates asymmetric cell division in invertebrates (Afshar et al., 2004; Couwenbergs et
162 al., 2004; David et al., 2005; Hampoelz et al., 2005; Wang et al., 2005), we observed no significant
163 defects in mitotic spindle orientation at the ventricular surface. Additionally, no ectopic expression of
164 neural crest markers or Wnt pathway activation was observed (**Supplemental Fig. 7**). Altogether, these
165 results further indicate that non-neural-cell deficiency is responsible for ectopia formation in *ric8a*
166 mutants.

167

168 **Microglial *ric8a* deficiency is responsible for ectopia formation**

169 To assess the role of non-neural cell types, we turned our attention to microglia since RNA-seq studies
170 show that brain microglia express *emx1* at a significant level (Zhang et al., 2014). To determine if *emx1-*
171 *cre* is expressed and active in microglia, we isolated microglia from *ric8a-emx1-cre* mutants. We found
172 that *emx1-cre* mediated *ric8a* deletion indeed resulted in altered cytokine expression in microglia
173 (**Supplemental Fig. 8**). This indicate that *emx1-cre* is expressed and active in microglia and deletes *ric8a*.

174 To determine the specific significance of *ric8a* deletion from microglia alone, we next employed a
175 microglia-specific *cx3cr1-cre* (Yona et al., 2013). Like *emx1-cre* mutants, *ric8a-cx3cr1-cre* mutant
176 microglia also showed elevated cytokine secretion and transcription in comparison to control microglia
177 upon stimulation by lipopolysaccharide (LPS) (**Fig. 2a-b**). Similar results were also obtained with
178 stimulation by polyinosinic-polycytidylic acid (poly I:C), an intracellular immune activator. Thus, these
179 results indicate that *ric8a* deficiency in microglia results in broad increases in microglial sensitivity to
180 immune stimulation.

181

182 To determine if microglial *ric8a* deficiency alone is sufficient to cause cortical ectopia in vivo, we
183 examined *ric8a-cx3cr1-cre* mutants but found that it did not affect either basement membrane integrity
184 or cortical layering (**Fig. 2c**). We reasoned that this may be related to the fact that *ric8a* mutant
185 microglia only show heightened activity upon stimulation but not under basal unstimulated conditions
186 (**Fig. 2a-b**) but elevated microglial activity may be needed for basement membrane degradation and
187 ectopia formation. To test this possibility, we employed in utero LPS administration to activate microglia
188 during cortical development. We found that over 50% of *ric8a-cx3cr1-cre* mutant neonates showed
189 ectopia when administered LPS at E11.5-12.5 (10 of 19 mutant neonates examined) (**Fig. 2d**). In
190 contrast, no cortical ectopia were observed in any of the 32 littermate controls that were similarly
191 administered LPS. This indicates that only the combination of microglial *ric8a* deficiency and immune
192 activation leads to ectopia formation. In *emx1-cre* mutants, ectopia develop without LPS administration
193 (**Fig. 1**). We suspect that this may be due to concurrent *ric8a* deficiency in neural cell types, which may
194 result in deficits that mimic immune stimulation. To test this, we next additionally deleted *ric8a* from
195 neural cells in the *ric8a-cx3cr1-cre* microglial mutant background by introducing *nestin-cre*. We have
196 shown that *ric8a* deletion by *nestin-cre* alone does not result in ectopia (**Fig. 1g-g'**). However, we found

197 that, like deletion by *emx1-cre*, *ric8a* deletion by the dual *cre* combination of *cx3cr1-cre* and *nestin-cre*
198 also resulted in ectopia in all double *cre* mutants (6 of 6 examined) (**Fig. 2f**). Thus, these results indicate
199 that elevated immune activation of *ric8a* deficient microglia during cortical development is responsible
200 for ectopia formation.

201

202 **Microglial *app* deficiency also results in ectopia formation**

203 The exclusive localization of ectopia to the lateral cortex in *ric8a* mutants is reminiscent of the
204 phenotypes observed in APP family and pathway mutants including *app/aplp1/2* triple (Herms et al.,
205 2004) and *apbb1/2* double knockouts (Guenette et al., 2006). Independent studies also point to a role
206 of non-neural cells in ectopia formation in these mutants. For example, unlike the triple knockout,
207 specific *app* knockdown in cortical neurons during development results in under- but not over-migration
208 of neurons (Young-Pearse et al., 2007). To test the role of microglia in ecotopia formation in APP
209 pathway mutants, we first analyzed *app* mutant microglia. To this end, we employed *cx3cr1-cre* to
210 delete a conditional allele of *app* from microglia and found that microglia cultured from *app-cx3cr1-cre*
211 mutants showed reduced TNFα and IL-6 secretion as well as muted IL-6 transcription upon stimulation
212 (**Fig. 3a, Supplemental Fig. 9**). This indicates that *app* plays a previously unrecognized, cell-autonomous
213 role in microglia in regulating microglial activity. Microglia exhibit attenuated immune response
214 following chronic stimulation, especially when carrying strong loss-of-function mutations in anti-
215 inflammatory pathways (Chamberlain et al., 2015; Sayed et al., 2018). We suspect that the attenuated
216 response by *app* mutant microglia may result from similar effects following in vitro culture. To test
217 effects of *app* mutation under conditions that more closely resemble in vivo conditions, we next isolated
218 fresh, unelicited peritoneal macrophages and acutely analyzed their response to immune stimulation.
219 We found that *app* mutant macrophages showed significantly elevated secretion of all cytokines tested

220 (**Fig. 3b**). At the transcriptional level, mRNA induction was also increased for all cytokines (**Fig. 3c**).
221 Thus, like that of *ric8a*, the normal function of *app* also appears to be to suppress the inflammatory
222 activation of microglia.

223

224 To determine if microglial *app* deficiency is also responsible for ectopia formation in *app* triple
225 knockout mutants, we next asked if activating microglia in microglia-specific *app* mutants similarly
226 results in pial ectopia during cortical development. To this end, we administered LPS in utero at E11.5-
227 12.5 to *app-cx3cr1-cre* mutant animals as we did to *ric8a-cx3cr1-cre* mutants above. We found that,
228 while none of the 81 littermate controls administered LPS showed ectopia, a significant number of
229 mutant neonates showed ectopia (6 of 31 neonates examined, ~19%) (**Fig. 3e**). Thus, *app* deficient
230 microglia, when activated, also results in cortical ectopia during development. The reduced severity of
231 the ectopia observed, as compared to that in *ric8a/cx3cr1-cre* mutants, likely in part results from the
232 reduced LPS dosage (by ~3 folds) we had to use in these animas due to the enhanced immune sensitivity
233 of their strain genetic background. Other *app* gene family members are also expressed in microglia
234 (Zhang et al., 2014) and may in addition compensate for the loss of APP. Thus, these results indicate
235 that *app* normally plays a cell-autonomous role in microglia that negatively regulate microglial activation
236 and its loss of function underlies ectopia formation. The similarities between *app* and *ric8a* mutant
237 phenotypes suggest that they form a previously unknown anti-inflammatory pathway in microglia.

238

239 **Monomeric Aβ suppresses microglial inflammatory activation via APP and Ric8a**

240 The possibility that *app* and *ric8a* may form a novel anti-inflammatory pathway in microglia raises
241 questions on the identity of the ligands for the pathway. Several molecules have been reported to bind

242 to APP and/or activate APP-dependent pathways (Fogel et al., 2014; Milosch et al., 2014; Rice et al.,
243 2012), among which Aβ is note-worthy for its nanomolar direct binding affinity (Fogel et al., 2014;
244 Shaked et al., 2006). Aβ oligomers and fibrils have been shown by numerous studies to be pro-
245 inflammatory, while non-fibrillar Aβ lack such activity (Halle et al., 2008; Huang, 2023, 2024; Lorton et
246 al., 1996; Muehlhauser et al., 2001; Tan et al., 1999). In contrast, when employed under conditions that
247 favor the monomer conformation, Aβ inhibits T cell activation (Grant et al., 2012). This suggests that,
248 unlike Aβ oligomers, Aβ monomers may be anti-inflammatory. To test this possibility, we dissolved
249 Aβ40 peptides in DMSO, which has been shown to preserve the monomeric conformation (LeVine,
250 2004; Stine et al., 2011). We found that Aβ monomers as prepared potently suppressed the secretion of
251 large numbers of cytokines (**Fig. 4a**, **Supplemental Fig. 10**) and showed similar effects on microglia no
252 matter if they were activated by LPS or poly I:C (**Fig. 4b**). We also found that the Aβ monomers similarly
253 strongly inhibited the induction of cytokines at the transcriptional level (**Fig. 4c, Supplemental Fig. 10**).
254 In addition, we observed these effects with Aβ40 peptides from different commercial sources. Thus,
255 these results indicate that monomeric Aβ possesses a previously unreported anti-inflammatory activity
256 against microglia that strongly inhibits microglial inflammatory activation.

257

258 To determine whether monomeric Aβ signals through APP, we employed *app-cx3cr1-cre* mutant
259 microglia. We found that, unlike that of control microglia, Aβ monomers failed to suppress the
260 secretion of all tested cytokines by *app* mutant microglia (**Fig. 4d, Supplemental Fig. 10**). Interestingly,
261 this blockade appeared to be specific to *app* since Aβ monomers still significantly suppressed cytokine
262 secretion by *aplp2* mutant microglia. At the transcriptional level, Aβ monomers also failed to suppress
263 cytokine induction in *app* mutant microglia (**Fig. 4e, Supplemental Fig. 10**). Together, these results
264 indicate that APP is functionally required in microglia for Aβ monomer inhibition of cytokine expression

265 at both transcriptional and post-transcriptional levels. Cultured microglia from *app-cx3cr1*-cre mutants
266 showed attenuated immune activation (**Fig. 3**). To assess whether this may affect the efficacy of Aβ
267 monomer inhibition, we next tested the response of fresh, unelicited macrophages. We found that, like
268 that of control microglia, cytokine secretion by control macrophages was also strongly suppressed by Aβ
269 monomers (**Fig. 4f, Supplemental Fig. 10**). However, even though *app* mutant macrophages showed
270 elevated response to immune stimulation in comparison to control macrophages, they still failed to
271 respond to Aβ monomers and displayed levels of cytokine secretion that were indistinguishable from
272 those of DMSO-treated cells (**Fig. 4f, Supplemental Fig. 10**). Thus, these results further indicate that
273 APP function is required in microglia for mediating the anti-inflammatory effects of Aβ monomers.

274

275 The similarity of *ric8a* ectopia to *app* ectopia phenotype (**Figs. 2** & **3**) also suggests that Ric8a
276 functions in the same pathway as APP in mediating Aβ monomer anti-inflammatory signaling in
277 microglia. This is consistent with previous studies showing that heterotrimeric G proteins are coupled to
278 APP and mediate APP intracellular signaling in vitro and vivo (Fogel et al., 2014; Milosch et al., 2014;
279 Nishimoto et al., 1993; Ramaker et al., 2013) and that Ric8a is a molecular chaperone essential for the
280 post-translational stability of heterotrimeric G proteins (Gabay et al., 2011; Tall et al., 2003). To directly
281 test if Ric8a is part of this pathway, we next employed *ric8a-cx3cr1-cre* mutant microglia. We found
282 that, indeed, like that of *app* mutant microglia, Aβ monomers also failed to suppress the secretion of
283 TNFα and IL-6 by *ric8a* mutant microglia (**Fig. 4g**). This indicates that heterotrimeric G proteins function
284 is likely required in the same pathway of APP in microglia for the suppression of TNFα and IL-6 secretion.
285 However, unlike APP, we found that Ric8a appears to be dispensable for Aβ monomer regulation of
286 other cytokines. For example, unlike that of TNFα and IL-6, Aβ monomers still suppressed IL-1β
287 secretion by *ric8a* mutant microglia (**Supplemental Fig. 10**). It also appears to be dispensable for the

288 regulation of cytokine transcription since Aβ monomers similarly suppressed IL-6 transcriptional
289 induction in both control and *ric8a* mutant microglia. These results suggest that heterotrimeric G
290 proteins function may only mediate some of the anti-inflammatory signaling of monomeric Aβ. Thus,
291 APP and Ric8a-regulated heterotrimeric G proteins form part of a novel anti-inflammatory pathway
292 activated by monomeric Aβ in microglia.
293
294 **Elevated matrix metalloproteinases (MMPs) cause basement membrane degradation**

295 We have shown that heightened microglial activation due to mutation in the Aβ monomer-activated
296 APP/Ric8a pathway results in basement membrane degradation and ectopia during cortical
297 development. To further test this interpretation, we sought to test the prediction that inhibition of
298 microglial activation in these mutants suppressed the formation ectopia. To this end, we employed
299 dorsomorphin and S3I-201, inhibitors targeting Akt, Stat3, and other mediators in pro-inflammatory
300 signaling (Lee et al., 2016; Qin et al., 2012). Consistent with their anti-inflammatory activity, we found
301 that dorsomorphin and S3I-201 both suppressed astrogliosis associated with neuroinflammation in the
302 cortex of *ric8a-emx1-cre* mutants (**Supplemental Fig. 11**). Furthermore, they also suppressed the
303 formation of ectopia in *ric8a-emx1-cre* mutants, reducing both the number and the size of the ectopia
304 observed (**Fig. 5a-f**). Most strikingly, the combined administration of dorsomorphin and S3I-201 nearly
305 eliminated all ectopia in *ric8a-emx1-cre* mutants (**Fig. 5d, 5e**). Thus, these results indicate that excessive
306 inflammatory activation of microglia is responsible for ectopia formation in *ric8a* mutants.
307
308 Under neuroinflammatory conditions, brain cytokines frequently induce MMPs, which lead to
309 breakdown of the extracellular matrix and contribute to disease pathology (Pagenstecher et al., 1998;
310 Wang et al., 2000). Since *ric8a* mutant microglia are hyperactive in inflammatory cytokine production,

311 we wonder if induction of MMPs may underlie the laminin degradation and cortical basement
312 membrane break observed in *ric8a* mutants. To test this, we examined the activities of MMP2 and
313 MMP9 in the developing cortex using gelatin gel zymography. We found that the activity of MMP9 in
314 the mutant cortex was significantly increased (**Fig. 5i, Supplemental Fig. 12**). In contrast, that activity of
315 MMP2 remained unaffected. Similarly, at the protein level, we found that the immunoreactivity for
316 MMP9 was increased in *ric8a-emx1-cre* mutants (**Fig. 5g-h**). To test if the increased MMP activity is
317 responsible for the ectopia observed, we next employed BB94, a broad-spectrum inhibitor of MMPs.
318 We found that BB94 administration significantly suppress both the number and the size of the ectopia in
319 *ric8a* mutants (**Fig. 5j-m**). To narrow down the identity of MMPs responsible, we further employed an
320 inhibitor specific for MMP9 and 13 and found that it similarly suppressed both the number and the size
321 of the ectopia (**Fig. 5l-m**). Furthermore, consistent with its near complete suppression of cortical
322 ectopia (**Fig. 5a-f**), we found that the co-administration of dorsomorphin and S3I-201 also reduced
323 MMP9 activity in the mutant cortex to the control level (**Supplemental Fig. 12**). Thus, these results
324 indicate this Aβ monomer-activated anti-inflammatory pathway normally promotes cortical
325 development through suppressing microglial activation and MMP induction.

326

327

328 **DISCUSSION**

329 The spatiotemporal expression of immune cytokines by glial cells in the brain plays critical roles in the
330 normal development, function, and plasticity of the brain circuitry (Barres, 2008; Schafer and Stevens,
331 2015; Zipp et al., 2023). In this article, we have identified a novel microglial anti-inflammatory pathway
332 activated by monomeric Aβ that inhibits microglial cytokine expression and plays essential roles in the
333 normal development of the cerebral cortex. We have found that this pathway is mediated by APP and
334 heterotrimeric G proteins in microglia and its activation leads to the inhibition of microglial cytokine
335 induction at transcriptional and post-transcriptional levels (**Figs. 1-4**). We further show that a key
336 function of this pathway is to suppress the activity of MMP9 during corticogenesis and disruption of this
337 regulation results in cortical basement membrane degradation and neuronal ectopia development (**Figs.**
338 **1-3, 5**). Furthermore, we find that this pathway is activated specifically by the monomeric form of Aβ
339 (**Fig. 4**), identifying, for the first time, an isoform specific activity of Aβ against microglia. These results
340 provide novel insights into the neuron-glia communication mechanisms that coordinate the regulation
341 of immune cytokines, key regulators of Hebbian and non-Hebbian synaptic plasticity, by glial cells in the
342 brain. The discovery of the novel activity of monomeric Aβ as a negative microglial regulator may also
343 facilitate the further elucidation of Alzheimer's disease pathogenesis.

344

345 **Microglial activity regulation during cortical development**

346 Among the glial cell populations in the brain, astrocytes and oligodendrocyte are both born within the
347 nervous system at the end of cortical neurogenesis. As such, they play limited roles in the early steps of
348 cortical development. In contrast, microglia are not only of a distinct non-neural lineage that originates
349 from outside the nervous system but also begin to populate the brain at the onset of corticogenesis
350 (Ginhoux et al., 2010; Hattori et al., 2023). As such, they play unique roles throughout cortical

351 development. Indeed, microglial activity has been found to regulate the size of the cortical neural
352 precursor pool (Cunningham et al., 2013). Microglia-secreted cytokines have also been found to
353 promote both neurogenesis and oligodendrogenesis (Shigemoto-Mogami et al., 2014). As such, the
354 precise regulation of microglial activity is critical to the normal development of the neocortex from an
355 early stage. In this study, we have shown that immune over-activation of microglia due to disruption of
356 a monomeric Aβ-activated pathway results in excessive cortical matrix proteinase activation, leading
357 basement membrane degradation and neuronal ectopia. Previous studies have shown that reductions
358 in the expression of microglial immune and chemotaxis genes instead lead to the failure of microglia to
359 populate the brain (Iyer et al., 2022). These results together thus highlight the importance of precisely
360 regulating the level of microglial activity during brain development. The dramatic destructive effects of
361 microglial hyperactivity we have observed during corticogenesis also foreshadow the critical roles it
362 plays in brain dysfunction and disease at later stages of life.

363

364 In this study, we have also shown that the anti-inflammatory regulation of microglia in
365 corticogenesis depends on a pathway composed of APP and Ric8a-regulated heterotrimeric G proteins.
366 This has revealed new insight into the intercellular signaling mechanisms regulating microglial activity in
367 the brain. Heterotrimeric G proteins are well-known mediators of G protein-coupled receptor (GPCR)
368 signaling. In this study, we have found that they also function in the same pathway as APP. To our
369 knowledge, ours is the first study to report an in vivo anti-inflammatory function of this pathway in
370 microglia and has significantly advanced knowledge in microglial biology. This is also consistent with
371 previous studies showing that heterotrimeric G proteins interact with the APP cytoplasmic domain and
372 mediate APP signaling from invertebrates to mammals in several other cell types (Fogel et al., 2014;
373 Milosch et al., 2014; Nishimoto et al., 1993; Ramaker et al., 2013). In this study, we have in addition

374 shown that this pathway is specifically activated by the monomeric form of Aβ, a peptide produced by
375 neurons in the brain (Cirrito et al., 2005), providing further insight into the biological function of this
376 pathway. In the early cortex, neurogenesis is just beginning, and most neurons born are in an immature
377 state. It is unclear if this pathway is activated by Aβ at this stage. However, studies have shown that
378 other APP ligands such as pancortin, a member of the olfactomedin family proteins known to inhibit
379 innate immunity (Liu et al., 2010), are expressed in the cortex at this stage (Rice et al., 2012). It will be
380 interesting to determine if these innate immune regulators play a role in regulating this pathway.

381

382 **Neuronal activity, glial cytokine expression, and brain circuit plasticity**

383 Activity-dependent competitive and homeostatic plasticity is a foundational rule that regulates the
384 development, maturation, and function of neural circuits across brain regions. Studies have shown that
385 glial cells, through regulating the spatiotemporal expression of immune cytokines, play a pivotal role in
386 this process. In the developing thalamus, by activating interleukin-33 expression in an activity-
387 dependent manner, astrocytes have been found to promote the segregation of eye-specific axonal
388 projection and the maturation of the visual circuitry (He et al., 2022; Vainchtein et al., 2018). In the
389 visual cortex, astrocytic expression of TNFα similarly mediates activity-dependent homeostatic upscaling
390 of cortical synapses following peripheral monocular deprivation (Barnes et al., 2017; Heir et al., 2024;
391 Kaneko et al., 2008). In this study, we have shown that Aβ monomers inhibit expression of cytokines by
392 brain microglia via a novel APP/heterotrimeric G protein-mediated pathway. Aβ is primarily produced
393 by neurons in the brain in a neural activity-dependent manner and form oligomers when large quantities
394 are produced (Cirrito et al., 2005). Aβ oligomers, in contrary to monomers, are proinflammatory and
395 increase glial cytokine expression (Halle et al., 2008; Huang, 2023; Lorton et al., 1996; Muehlhauser et
396 al., 2001; Tan et al., 1999). These findings thus suggest that different levels of neural circuit activity in

397 the brain may differentially regulate glial cytokine expression through inducing different levels of Aβ.
398 High levels of neural activity may lead to high levels of Aβ and the formation of Aβ oligomers that
399 activate glial cytokine production, while low levels of neural activity may produce low levels of Aβ,
400 maintain Aβ as monomers, and inhibit glial cytokine production. Thus, Aβ in the brain may not only be a
401 reporter of the levels of neural circuit activity but may also serve as an agent that directly mediate
402 activity level-dependent plasticity. Following sensory deprivation, for example, Aβ levels may be
403 lowered due to loss of sensory stimulation. This may lead to the relief of monomeric Aβ inhibition of
404 cytokines such as TNFα and as a result trigger homeostatic upscaling of cortical synapses in the visual
405 cortex (Barnes et al., 2017; Heir et al., 2024; Kaneko et al., 2008). In contrary, when neural activity levels
406 are high, large quantities of Aβ may be produced, leading to formation of Aβ oligomers that may in turn
407 induce expression of cytokines such as IL-33 that promote synaptic pruning. A large body of evidence
408 strongly indicates that Aβ and related pathways indeed mediate homeostatic and competitive plasticity
409 in the visual and other systems of the brain (Galanis et al., 2021; Huang, 2023, 2024; Kamenetz et al.,
410 2003; Kim et al., 2013). Our discovery of the Aβ monomer-activated pathway has therefore provided
411 novel insights into a universal mechanism that senses neural circuit activity pattern and translates it into
412 homeostatic and competitive synaptic changes in the brain, a mechanism with fundamental roles in
413 cognitive function.

414

415 In this study, we have also found that the matrix proteinase MMP9 is a key downstream effector
416 of microglial activity in the developing cortex. We find that microglial hyperactivity results in increased
417 levels of MMP9, leading to cortical basement membrane degradation and neuronal ectopia and
418 inhibiting MMP9 directly or indirectly suppresses the phenotype. This suggests that the regulation of
419 MMP9 may be a key mechanism by which glial cells regulate brain development and plasticity. Indeed,

420 independent studies have shown that, in the visual cortex, MMP9 is also a pivotal mediator of TNFα-
421 dependent homeostatic upscaling of central synapses following monocular deprivation (Akol et al.,
422 2022; Kaneko et al., 2008; Kelly et al., 2015; Spolidoro et al., 2012). In the Xenopus tectum, MMP9 has
423 similarly been found to be induced by neural activity and promote visual activity-induced dendritic
424 growth (Gore et al., 2021). Importantly, in both wildtype and amblyopic animals, light reintroduction
425 after dark exposure has been found to reactivate plasticity in the adult visual cortex via MMP9,
426 uncovering a potential treatment for common visual conditions (Murase et al., 2017; Murase et al.,
427 2019). These results therefore highlight a conserved glia/cytokine/MMP9-mediated mechanism that
428 regulates brain development and plasticity from embryogenesis to adulthood. In ocular dominance
429 plasticity, MMP9 is activated at perisynaptic regions (Murase et al., 2017; Murase et al., 2019). MMP9
430 mRNA translation has been also observed in dendrites (Dziembowska et al., 2012). In the *ric8a* mutant
431 cortex, we find that MMP9 activity is increased. Further studies are required to determine the cellular
432 sources of MMP9 and how its activity is regulated.

433

434 **Aβ monomer anti-inflammatory activity and Alzheimer's disease**

435 Aβ is well known as a component of the amyloid plaques in the Alzheimer's disease brain. It is a unique
436 amphipathic peptide that can, dependent on concentration and other conditions, remain as monomers
437 or form oligomers. Studies on Aβ have historically focused on the neurotoxic effects of Aβ oligomers
438 and their proinflammatory effects on glia (Gulisano et al., 2018; Halle et al., 2008; He et al., 2019;
439 Huang, 2023; Kim et al., 2013; Lauren et al., 2009; Lazarevic et al., 2017; Lorton et al., 1996;
440 Muehlhauser et al., 2001; Parodi et al., 2010; Puzzo et al., 2008; Shankar et al., 2008; Tan et al., 1999;
441 Walsh et al., 2002; Yang et al., 2015; Zott et al., 2019). In this study, we have found that, in contrary to
442 Aβ oligomers, Aβ monomers instead possess a previously unknown anti-inflammatory activity that acts

443 through a unique microglial pathway. We have further found that genetic disruption of this pathway in
444 corticogenesis results microglial hyperactivity, leading to neuronal ectopia and large disruption of
445 cortical structural organization. To our knowledge, ours is the first study to uncover this overlooked
446 anti-inflammatory activity of Aβ monomers. It is in alignment with recent studies showing that Aβ
447 monomers are also directly protective to neurons and positively regulate synapse development and
448 function (Galanis et al., 2021; Giuffrida et al., 2009; Plant et al., 2003; Ramsden et al., 2002; Zhou et al.,
449 2022). Assuming a set amount of Aβ peptides, the formation of Aβ oligomers and aggregates in the
450 brain would, by chemical law, be predicted to result in the depletion of Aβ monomers (Dear et al., 2020;
451 Michaels et al., 2020). Thus, in the Alzheimer's disease brain, besides the obvious formation of Aβ
452 aggregates, there may also be a less visible depletion of Aβ monomers taking place at the same time,
453 which may, like Aβ oligomers, also contribute to the development of neuroinflammation and neuronal
454 damage (Huang, 2023). In support of this interpretation, high soluble brain Aβ42, which likely also
455 means high levels of Aβ monomers in the brain, have been found in clinical studies to preserve cognition
456 in patients of both familial and sporadic Alzheimer's disease, in spite of increasing amyloidosis detected
457 in their brains (Espay et al., 2021; Sturchio et al., 2022; Sturchio et al., 2021). In our study, we have also
458 found that the effects of microglial disinhibition are mediated by MMP9. Importantly, in
459 neurodegenerative diseases, MMP9 has been similarly found to be a key determinant regulatings the
460 selective degeneration of neuronal cell types (Kaplan et al., 2014; Tran et al., 2019). MMP9 levels are
461 also upregulated in the plasma in both mild cognitive impairment and Alzheimer's disease patients
462 (Bruno et al., 2009; Lorenzl et al., 2008; Tsiknia et al., 2022). In addition, in several motor neuron
463 disease models, reducing MMP9 has been found to protect neurons and delay the loss of motor
464 function (Kaplan et al., 2014; Spiller et al., 2019). Thus, our study has not only uncovered a potentially
465 overlooked role of Aβ monomer depletion in the development of Alzheimer's disease but also identified

466 downstream effectors. Elucidating the roles these factors play may reveal new insight into the

467 pathogenesis of Alzheimer's disease.

468

469

470 **METHODS**

471 **Generation of *ric8a* conditional allele**

472 Standard molecular biology techniques were employed for generating the conditional *ric-8a* allele.
473 Briefly, genomic fragments, of 4.5 and 2.5 kilobases and flanking exons 2-4 of the *ric-8a* locus at the 5'
474 and 3' side, respectively, were isolated by PCR using high fidelity polymerases. Targeting plasmid was
475 constructed by flanking the genomic fragment containing exons 2-4 with two loxP sites together with a
476 *neomycin* positive selection cassette, followed by 5' and 3' genomic fragments as homologous
477 recombination arms and a *pgk-DTA* gene as a negative selection cassette. ES cell clones were screened
478 by Southern blot analysis using external probes at 5' and 3' sides. For derivation of conditional allele, the
479 *neomycin* cassette was removed by crossing to an *actin-flpe* transgenic line after blastocyst injection and
480 germ line transmission. The primer set for genotyping *ric-8a* conditional allele, which produces a
481 wildtype band of ~110bp and a mutant band of ~200bp, is: 5'- cctagttgtgaatcagaagcacttg-3' and 5'-
482 gccatacctgagttacctaggc-3'. Animals homozygous for the conditional *ric-8a* allele are viable and fertile,
483 without obvious phenotypes.

484

485 **Mouse breeding and pharmacology**

486 *emx1-cre, nestin-cre, foxg1-cre, cx3cr1-cre, floxed app* as well as the *BAT-lacZ* reporter mouse lines were
487 purchased from the Jackson Lab. *nex-cre* and *wnt3a-cre* were as published (Goebbels et al., 2006; Yoshida
488 et al., 2006). *cre* transgenes were introduced individually into the *ric8a or app* conditional mutant
489 background for phenotypic analyses and *ric8a or app* homozygotes without *cre* as well as heterozygotes
490 with *cre* (littermates) were both analyzed as controls. For BB94 and MMP9/13 inhibitor injection, pregnant
491 females were treated daily from E12.5 to E14.5 at 30 μg (BB94) or 37.5 μg (MMP9/13 inhibitor) per g of

492 body weight. For dorsomorphin and S3I-201 injection, pregnant females were treated on E12.5 at 7.5 and 25
493 μg per g of body weight, respectively. For sham treatment, pregnant females were treated on E12.5 with
494 100 μls of DMSO. BrdU was injected at 100 μg per g of body weight, and embryos were collected 4 hours
495 later for cell proliferation analysis, or alternatively, pups were sacrificed at P5 for neuronal migration
496 analysis and at P17 for other analysis. For LPS treatment, pregnant females were injected intraperitoneally
497 with 400ng (*ric8a* genetic background) or 150ng (*app* genetic background) LPS per g of body weight on both
498 E11.5 and E12.5. Animal use was in accordance with institutional guidelines.

499

500 **Immunohistochemistry**

501 Vibratome sections from brains fixed in 4% paraformaldehyde were used. The following primary antibodies
502 were used at respective dilutions/concentrations: mouse anti-BrdU supernatant (clone G3G4,
503 Developmental Studies Hybridoma Bank (DSHB), University of Iowa, IA; 1:40), mouse anti-RC2 supernatant
504 (DSHB; 1:10), mouse anti-Nestin supernatant (DSHB; 1:20), mouse anti-Vimentin supernatant (DSHB; 1:10),
505 mouse anti-Pax6 supernatant (DSHB; 1:20), moue anti-Reelin (Millipore, 1:500), mouse anti-chondroitin
506 sulfate (CS-56, Sigma, 1:100), rat anti-Ctip2 (Abcam, 1:500), rabbit anti-phospho Histone H3 (Ser10)
507 (Millipore; 1:400), rabbit anti-Cux1 (CDP) (Santa Cruz; 1:100), rabbit anti-laminin (Sigma; 1:2000), rabbit anti-
508 GFAP (Dako;1:1000), rabbit anti-ALDH1L1 (Abcam, 1:500), rabbit anti-MMP9 (Abcam, 1:1000), goat anti-
509 MMP2 (R&D Systems; 5 μg/ml), rabbit anti-Calretinin (Chemicon, 1:2000), mouse anti-S100β (Thermo
510 Scientific; 1:100), rabbit anti-S100β (Thermo Scientific; 1:200), and rabbit anti-phospho-Smad1/5
511 (Ser463/465) (41D10; Cell Signaling, 1:200). FITC and Cy3 conjugated secondary antibodies were purchased
512 from Jackson ImmunoResearch Laboratories (West Grove, PA). Peroxidase conjugated secondary antibodies
513 were purchased from Santa Cruz Biotech. Staining procedures were performed as described previously
514 (Huang et al., 2006), except for anti-Ric-8a, MMP9, and phospho-Smad1/5 staining, in which a tyramide

515 signal amplification (TSA) plus Cy3 kit (PerkinElmer, Waltham, MA) was used per manufacturer's instruction.
516 Sections were mounted with Fluoromount G medium (Southern Biotech, Birmingham, AB) and analyzed
517 under a Nikon *eclipse* Ti microscope or an Olympus confocal microscope.

518

519 **Microglia culture and assay**

520 Cerebral hemispheres were dissected from individual neonates, mechanically dissociated, split into 3-4
521 wells each and cultured in DMEM-F12 (Lonza) containing 10% fetal bovine serum (FBS) (Invitrogen).
522 Microglial cells were harvested by light trypsinization that removes astroglial sheet on day 13-15. For
523 experiments other than assaying IL-1β secretion, microglia were treated with LPS at 20ng/ml for 3 hours
524 or at 5ng/ml overnight and, if applicable, DMSO or Aβ40 (ApexBio and Genscript) was applied at the
525 same time as LPS. For assaying IL-1β secretion, microglia were primed with LPS at 200ng/ml for 5-6
526 hours before treatment with 3mM ATP for 15 minutes. In these experiments, DMSO or Aβ40 was
527 applied at the same time as ATP if applicable. Supernatants were collected and used for cytokine ELISA
528 assays per manufacturer's instructions (Biolegend). Total RNAs were prepared from collected cells using
529 Trizol (Invitrogen) and cDNAs were synthesized using a High-capacity cDNA reverse transcription kit
530 (Applied Biosystems). Quantitative PCR was performed using a GoTaq qPCR master mix per
531 manufacturer's instructions (Promega). All gene expression levels were normalized against that of
532 GAPDH.

533

534 **Quantitative and statistical analysis**

535 The sample size was estimated to be 3-9 animals each genotype (every 4th of 50 μm coronal sections, 7-
536 10 sections each animal) for ectopia analysis, 3-5 animals each genotype (3-4 sections each animal) for

537 immunohistochemical analysis, and 4-6 animals each genotype for gel zymography and Western blot
538 analysis, as has been demonstrated by previous publications to be adequate for similar animal studies.
539 Matching sections were used between controls and mutants. NIS-Elements BR 3.0 software (Nikon) was
540 used for quantifying the numbers and sizes of neuronal ectopia, the numbers of laminin positive debris,
541 as well as the numbers of astrocytes. ImageJ software (NIH) was used for quantifying the intensity of
542 immunostainings. Statistics was performed using Student's *t* test when comparing two conditions, or
543 one-way ANOVA followed by Tukey's post hoc test when comparing three or more conditions. All data
544 are represented as means $\pm$ s.e.m.

545

546 ## ACKNOWLEDGMENTS

547 Z. H. thanks Dr. L. F. Reichardt for supporting the initial generation of *ric8a* mutant ES cells, Dr. E. A.
548 Grove (Chicago) for providing the *wnt3a-cre* strain, the late Dr. B. A. Barres (Stanford) for critiques and
549 input, and Drs. W. L. Murphy and E. Bresnick (UW-Madison) for access to a plate reader and a qPCR
550 machine. We also thank the late Dr. D. Oertel (UW-Madison) for critical reading and editing and Dr. L
551 Puglielli (UW-Madison) for critical reading of a previous version of the manuscript. This work was
552 supported by funds from the Departments of Neurology and Neuroscience, UW-Madison, and a Basil
553 O'Connor award from the March of Dimes foundation to Z.H.

554

555 ## AUTHOR INFORMATION

556 Z. H. designed experiments, generated *ric8a* conditional ES cells, performed microglial and related
557 experiments, and wrote the manuscript. H. J. K., D. S., and Z. H. performed other experiments and
558 analyzed data.

559

560

561

562

563

564

565

566

567 **REFERENCES**

568

569 Afshar, K., Willard, F.S., Colombo, K., Johnston, C.A., McCudden, C.R., Siderovski, D.P., and Gonczy, P.
570 (2004). RIC-8 is required for GPR-1/2-dependent Galpha function during asymmetric division of C.
571 elegans embryos. Cell *119*, 219-230.

572 Akol, I., Kalogeraki, E., Pielecka-Fortuna, J., Fricke, M., and Lowel, S. (2022). MMP2 and MMP9 Activity Is
573 Crucial for Adult Visual Cortex Plasticity in Healthy and Stroke-Affected Mice. The Journal of
574 neuroscience : the official journal of the Society for Neuroscience *42*, 16-32.

575 Barnes, S.J., Franzoni, E., Jacobsen, R.I., Erdelyi, F., Szabo, G., Clopath, C., Keller, G.B., and Keck, T.
576 (2017). Deprivation-Induced Homeostatic Spine Scaling In Vivo Is Localized to Dendritic Branches that
577 Have Undergone Recent Spine Loss. Neuron *96*, 871-882 e875.

578 Barres, B.A. (2008). The mystery and magic of glia: a perspective on their roles in health and disease.
579 Neuron *60*, 430-440.

580 Beggs, H.E., Schahin-Reed, D., Zang, K., Goebbels, S., Nave, K.A., Gorski, J., Jones, K.R., Sretavan, D., and
581 Reichardt, L.F. (2003). FAK deficiency in cells contributing to the basal lamina results in cortical
582 abnormalities resembling congenital muscular dystrophies. Neuron *40*, 501-514.

583 Belvindrah, R., Nalbant, P., Ding, S., Wu, C., Bokoch, G.M., and Muller, U. (2006). Integrin-linked kinase
584 regulates Bergmann glial differentiation during cerebellar development. Molecular and cellular
585 neurosciences *33*, 109-125.

586 Bruno, M.A., Mufson, E.J., Wuu, J., and Cuello, A.C. (2009). Increased matrix metalloproteinase 9 activity
587 in mild cognitive impairment. J Neuropathol Exp Neurol *68*, 1309-1318.

588 Chamberlain, L.M., Holt-Casper, D., Gonzalez-Juarrero, M., and Grainger, D.W. (2015). Extended culture
589 of macrophages from different sources and maturation results in a common M2 phenotype. J Biomed
590 Mater Res A *103*, 2864-2874.

591 Cirrito, J.R., Yamada, K.A., Finn, M.B., Sloviter, R.S., Bales, K.R., May, P.C., Schoepp, D.D., Paul, S.M.,
592 Mennerick, S., and Holtzman, D.M. (2005). Synaptic activity regulates interstitial fluid amyloid-beta
593 levels in vivo. Neuron *48*, 913-922.

594 Colonna, M., and Butovsky, O. (2017). Microglia Function in the Central Nervous System During Health
595 and Neurodegeneration. Annu Rev Immunol *35*, 441-468.

596 Couwenbergs, C., Spilker, A.C., and Gotta, M. (2004). Control of embryonic spindle positioning and
597 Galpha activity by C. elegans RIC-8. Current biology : CB *14*, 1871-1876.

598 Cunningham, C.L., Martinez-Cerdeno, V., and Noctor, S.C. (2013). Microglia regulate the number of
599 neural precursor cells in the developing cerebral cortex. The Journal of neuroscience : the official journal
600 of the Society for Neuroscience *33*, 4216-4233.

601 David, N.B., Martin, C.A., Segalen, M., Rosenfeld, F., Schweisguth, F., and Bellaiche, Y. (2005). Drosophila
602 Ric-8 regulates Galphai cortical localization to promote Galphai-dependent planar orientation of the
603 mitotic spindle during asymmetric cell division. Nature cell biology *7*, 1083-1090.

604 Dear, A.J., Michaels, T.C.T., Meisl, G., Klenerman, D., Wu, S., Perrett, S., Linse, S., Dobson, C.M., and
605 Knowles, T.P.J. (2020). Kinetic diversity of amyloid oligomers. Proceedings of the National Academy of
606 Sciences of the United States of America *117*, 12087-12094.

607 Dziembowska, M., Milek, J., Janusz, A., Rejmak, E., Romanowska, E., Gorkiewicz, T., Tiron, A., Bramham,
608 C.R., and Kaczmarek, L. (2012). Activity-dependent local translation of matrix metalloproteinase-9. The
609 Journal of neuroscience : the official journal of the Society for Neuroscience *32*, 14538-14547.

610 Eichler, A., Kleidonas, D., Turi, Z., Fliegauf, M., Kirsch, M., Pfeifer, D., Masuda, T., Prinz, M., Lenz, M., and
611 Vlachos, A. (2023). Microglial Cytokines Mediate Plasticity Induced by 10 Hz Repetitive Magnetic
612 Stimulation. The Journal of neuroscience : the official journal of the Society for Neuroscience *43*, 3042-
613 3060.

614 Espay, A.J., Sturchio, A., Schneider, L.S., and Ezzat, K. (2021). Soluble Amyloid-beta Consumption in
615 Alzheimer's Disease. J Alzheimers Dis *82*, 1403-1415.

616 Fogel, H., Frere, S., Segev, O., Bharill, S., Shapira, I., Gazit, N., O'Malley, T., Slomowitz, E., Berdichevsky,
617 Y., Walsh, D.M.*, et al.* (2014). APP homodimers transduce an amyloid-beta-mediated increase in release
618 probability at excitatory synapses. Cell reports *7*, 1560-1576.

619 Gabay, M., Pinter, M.E., Wright, F.A., Chan, P., Murphy, A.J., Valenzuela, D.M., Yancopoulos, G.D., and
620 Tall, G.G. (2011). Ric-8 proteins are molecular chaperones that direct nascent G protein alpha subunit
621 membrane association. Science signaling *4*, ra79.

622 Galanis, C., Fellenz, M., Becker, D., Bold, C., Lichtenthaler, S.F., Muller, U.C., Deller, T., and Vlachos, A.
623 (2021). Amyloid-Beta Mediates Homeostatic Synaptic Plasticity. The Journal of neuroscience : the official
624 journal of the Society for Neuroscience *41*, 5157-5172.

625 Garcia-Osta, A., and Alberini, C.M. (2009). Amyloid beta mediates memory formation. Learn Mem *16*,
626 267-272.

627 Ginhoux, F., Greter, M., Leboeuf, M., Nandi, S., See, P., Gokhan, S., Mehler, M.F., Conway, S.J., Ng, L.G.,
628 Stanley, E.R.*, et al.* (2010). Fate mapping analysis reveals that adult microglia derive from primitive
629 macrophages. Science *330*, 841-845.

630 Giuffrida, M.L., Caraci, F., Pignataro, B., Cataldo, S., De Bona, P., Bruno, V., Molinaro, G., Pappalardo, G.,
631 Messina, A., Palmigiano, A.*, et al.* (2009). Beta-amyloid monomers are neuroprotective. The Journal of
632 neuroscience : the official journal of the Society for Neuroscience *29*, 10582-10587.

633 Goebbels, S., Bormuth, I., Bode, U., Hermanson, O., Schwab, M.H., and Nave, K.A. (2006). Genetic
634 targeting of principal neurons in neocortex and hippocampus of NEX-Cre mice. Genesis *44*, 611-621.

635 Gore, S.V., James, E.J., Huang, L.C., Park, J.J., Berghella, A., Thompson, A.C., Cline, H.T., and Aizenman,
636 C.D. (2021). Role of matrix metalloproteinase-9 in neurodevelopmental deficits and experience-
637 dependent plasticity in Xenopus laevis. eLife *10*.

638 Gorski, J.A., Talley, T., Qiu, M., Puelles, L., Rubenstein, J.L., and Jones, K.R. (2002). Cortical excitatory
639 neurons and glia, but not GABAergic neurons, are produced in the Emx1-expressing lineage. The Journal
640 of neuroscience : the official journal of the Society for Neuroscience *22*, 6309-6314.

641 Grant, J.L., Ghosn, E.E., Axtell, R.C., Herges, K., Kuipers, H.F., Woodling, N.S., Andreasson, K., Herzenberg,
642 L.A., Herzenberg, L.A., and Steinman, L. (2012). Reversal of paralysis and reduced inflammation from
643 peripheral administration of beta-amyloid in TH1 and TH17 versions of experimental autoimmune
644 encephalomyelitis. Sci Transl Med *4*, 145ra105.

645 Graus-Porta, D., Blaess, S., Senften, M., Littlewood-Evans, A., Damsky, C., Huang, Z., Orban, P., Klein, R.,
646 Schittny, J.C., and Muller, U. (2001). Beta1-class integrins regulate the development of laminae and folia
647 in the cerebral and cerebellar cortex. Neuron *31*, 367-379.

648 Guenette, S., Chang, Y., Hiesberger, T., Richardson, J.A., Eckman, C.B., Eckman, E.A., Hammer, R.E., and
649 Herz, J. (2006). Essential roles for the FE65 amyloid precursor protein-interacting proteins in brain
650 development. The EMBO journal *25*, 420-431.

651 Gulisano, W., Melone, M., Li Puma, D.D., Tropea, M.R., Palmeri, A., Arancio, O., Grassi, C., Conti, F., and
652 Puzzo, D. (2018). The effect of amyloid-beta peptide on synaptic plasticity and memory is influenced by
653 different isoforms, concentrations, and aggregation status. Neurobiol Aging *71*, 51-60.

654 Gulisano, W., Melone, M., Ripoli, C., Tropea, M.R., Li Puma, D.D., Giunta, S., Cocco, S., Marcotulli, D.,
655 Origlia, N., Palmeri, A.*, et al.* (2019). Neuromodulatory Action of Picomolar Extracellular Abeta42
656 Oligomers on Presynaptic and Postsynaptic Mechanisms Underlying Synaptic Function and Memory. The
657 Journal of neuroscience : the official journal of the Society for Neuroscience *39*, 5986-6000.

658 Halle, A., Hornung, V., Petzold, G.C., Stewart, C.R., Monks, B.G., Reinheckel, T., Fitzgerald, K.A., Latz, E.,
659 Moore, K.J., and Golenbock, D.T. (2008). The NALP3 inflammasome is involved in the innate immune
660 response to amyloid-beta. Nat Immunol *9*, 857-865.

661 Hampoelz, B., Hoeller, O., Bowman, S.K., Dunican, D., and Knoblich, J.A. (2005). Drosophila Ric-8 is
662 essential for plasma-membrane localization of heterotrimeric G proteins. Nat Cell Biol *7*, 1099-1105.

663 Hattori, Y., Kato, D., Murayama, F., Koike, S., Asai, H., Yamasaki, A., Naito, Y., Kawaguchi, A., Konishi, H.,
664 Prinz, M.*, et al.* (2023). CD206(+) macrophages transventricularly infiltrate the early embryonic cerebral
665 wall to differentiate into microglia. Cell reports *42*, 112092.

666 He, D., Xu, H., Zhang, H., Tang, R., Lan, Y., Xing, R., Li, S., Christian, E., Hou, Y., Lorello, P.*, et al.* (2022).
667 Disruption of the IL-33-ST2-AKT signaling axis impairs neurodevelopment by inhibiting microglial
668 metabolic adaptation and phagocytic function. Immunity *55*, 159-173 e159.

669 He, Y., Wei, M., Wu, Y., Qin, H., Li, W., Ma, X., Cheng, J., Ren, J., Shen, Y., Chen, Z.*, et al.* (2019). Amyloid
670 beta oligomers suppress excitatory transmitter release via presynaptic depletion of phosphatidylinositol-
671 4,5-bisphosphate. Nat Commun *10*, 1193.

672 Hebert, J.M., and McConnell, S.K. (2000). Targeting of cre to the Foxg1 (BF-1) locus mediates loxP
673 recombination in the telencephalon and other developing head structures. Developmental biology *222*,
674 296-306.

675 Heir, R., Abbasi, Z., Komal, P., Altimimi, H.F., Franquin, M., Moschou, D., Chambon, J., and Stellwagen, D.
676 (2024). Astrocytes Are the Source of TNF Mediating Homeostatic Synaptic Plasticity. The Journal of
677 neuroscience : the official journal of the Society for Neuroscience *44*.

678 Herms, J., Anliker, B., Heber, S., Ring, S., Fuhrmann, M., Kretzschmar, H., Sisodia, S., and Muller, U.
679 (2004). Cortical dysplasia resembling human type 2 lissencephaly in mice lacking all three APP family
680 members. The EMBO journal *23*, 4106-4115.

681 Huang, Z. (2023). A Function of Amyloid-beta in Mediating Activity-Dependent Axon/Synapse
682 Competition May Unify Its Roles in Brain Physiology and Pathology. J Alzheimers Dis *92*, 29-57.

683 Huang, Z. (2024). Evidence that Alzheimer's Disease Is a Disease of Competitive Synaptic Plasticity Gone
684 Awry. J Alzheimers Dis *99*, 447-470.

685 Huang, Z., Shimazu, K., Woo, N.H., Zang, K., Muller, U., Lu, B., and Reichardt, L.F. (2006). Distinct roles of
686 the beta 1-class integrins at the developing and the mature hippocampal excitatory synapse. J Neurosci
687 *26*, 11208-11219.

688 Iyer, H., Shen, K., Meireles, A.M., and Talbot, W.S. (2022). A lysosomal regulatory circuit essential for the
689 development and function of microglia. Sci Adv *8*, eabp8321.

690 Kamenetz, F., Tomita, T., Hsieh, H., Seabrook, G., Borchelt, D., Iwatsubo, T., Sisodia, S., and Malinow, R.
691 (2003). APP processing and synaptic function. Neuron *37*, 925-937.

692 Kaneko, M., Stellwagen, D., Malenka, R.C., and Stryker, M.P. (2008). Tumor necrosis factor-alpha
693 mediates one component of competitive, experience-dependent plasticity in developing visual cortex.
694 Neuron *58*, 673-680.

695 Kaplan, A., Spiller, K.J., Towne, C., Kanning, K.C., Choe, G.T., Geber, A., Akay, T., Aebischer, P., and
696 Henderson, C.E. (2014). Neuronal matrix metalloproteinase-9 is a determinant of selective
697 neurodegeneration. Neuron *81*, 333-348.

698 Kelly, E.A., Russo, A.S., Jackson, C.D., Lamantia, C.E., and Majewska, A.K. (2015). Proteolytic regulation of
699 synaptic plasticity in the mouse primary visual cortex: analysis of matrix metalloproteinase 9 deficient
700 mice. Front Cell Neurosci *9*, 369.

701 Kim, T., Vidal, G.S., Djurisic, M., William, C.M., Birnbaum, M.E., Garcia, K.C., Hyman, B.T., and Shatz, C.J.
702 (2013). Human LilrB2 is a beta-amyloid receptor and its murine homolog PirB regulates synaptic
703 plasticity in an Alzheimer's model. Science *341*, 1399-1404.

704 Lauren, J., Gimbel, D.A., Nygaard, H.B., Gilbert, J.W., and Strittmatter, S.M. (2009). Cellular prion protein
705 mediates impairment of synaptic plasticity by amyloid-beta oligomers. Nature *457*, 1128-1132.

706 Lazarevic, V., Fienko, S., Andres-Alonso, M., Anni, D., Ivanova, D., Montenegro-Venegas, C.,
707 Gundelfinger, E.D., Cousin, M.A., and Fejtova, A. (2017). Physiological Concentrations of Amyloid Beta
708 Regulate Recycling of Synaptic Vesicles via Alpha7 Acetylcholine Receptor and CDK5/Calcineurin
709 Signaling. Front Mol Neurosci *10*, 221.

710 Leathers, T.A., and Rogers, C.D. (2022). Time to go: neural crest cell epithelial-to-mesenchymal
711 transition. Development *149*.

712 Lee, Y., Park, B.H., and Bae, E.J. (2016). Compound C inhibits macrophage chemotaxis through an AMPK-
713 independent mechanism. Biochemical and biophysical research communications *469*, 515-520.

714 LeVine, H., 3rd (2004). Alzheimer's beta-peptide oligomer formation at physiologic concentrations. Anal
715 Biochem *335*, 81-90.

716 Lewitus, G.M., Konefal, S.C., Greenhalgh, A.D., Pribiag, H., Augereau, K., and Stellwagen, D. (2016).
717 Microglial TNF-alpha Suppresses Cocaine-Induced Plasticity and Behavioral Sensitization. Neuron *90*,
718 483-491.

719 Liu, W., Yan, M., Liu, Y., Wang, R., Li, C., Deng, C., Singh, A., Coleman, W.G., Jr., and Rodgers, G.P. (2010).
720 Olfactomedin 4 down-regulates innate immunity against Helicobacter pylori infection. Proceedings of
721 the National Academy of Sciences of the United States of America *107*, 11056-11061.

722 Lorenzl, S., Buerger, K., Hampel, H., and Beal, M.F. (2008). Profiles of matrix metalloproteinases and
723 their inhibitors in plasma of patients with dementia. Int Psychogeriatr *20*, 67-76.

724 Lorton, D., Kocsis, J.M., King, L., Madden, K., and Brunden, K.R. (1996). beta-Amyloid induces increased
725 release of interleukin-1 beta from lipopolysaccharide-activated human monocytes. Journal of
726 neuroimmunology *67*, 21-29.

727 Ma, S., Kwon, H.J., and Huang, Z. (2012). Ric-8a, a guanine nucleotide exchange factor for heterotrimeric
728 G proteins, regulates bergmann glia-basement membrane adhesion during cerebellar foliation. The
729 Journal of neuroscience : the official journal of the Society for Neuroscience *32*, 14979-14993.

730 Ma, S., Santhosh, D., Kumar, T.P., and Huang, Z. (2017). A Brain-Region-Specific Neural Pathway
731 Regulating Germinal Matrix Angiogenesis. Developmental cell *41*, 366-381 e364.

732 Michaels, T.C.T., Saric, A., Curk, S., Bernfur, K., Arosio, P., Meisl, G., Dear, A.J., Cohen, S.I.A., Dobson,
733 C.M., Vendruscolo, M.*, et al.* (2020). Dynamics of oligomer populations formed during the aggregation of
734 Alzheimer's Abeta42 peptide. Nat Chem *12*, 445-451.

735 Milosch, N., Tanriover, G., Kundu, A., Rami, A., Francois, J.C., Baumkotter, F., Weyer, S.W., Samanta, A.,
736 Jaschke, A., Brod, F.*, et al.* (2014). Holo-APP and G-protein-mediated signaling are required for
737 sAPPalpha-induced activation of the Akt survival pathway. Cell death & disease *5*, e1391.

Moore, S.A., Saito, F., Chen, J., Michele, D.E., Henry, M.D., Messing, A., Cohn, R.D., Ross-Barta, S.E., Westra, S., Williamson, R.A.*, et al.* (2002). Deletion of brain dystroglycan recapitulates aspects of congenital muscular dystrophy. Nature *418*, 422-425.

Morley, J.E., Farr, S.A., Banks, W.A., Johnson, S.N., Yamada, K.A., and Xu, L. (2010). A physiological role for amyloid-beta protein:enhancement of learning and memory. J Alzheimers Dis *19*, 441-449.

Muehlhauser, F., Liebl, U., Kuehl, S., Walter, S., Bertsch, T., and Fassbender, K. (2001). Aggregation-Dependent interaction of the Alzheimer's beta-amyloid and microglia. Clin Chem Lab Med *39*, 313-316.

Murase, S., Lantz, C.L., and Quinlan, E.M. (2017). Light reintroduction after dark exposure reactivates plasticity in adults via perisynaptic activation of MMP-9. eLife *6*.

Murase, S., Winkowski, D., Liu, J., Kanold, P.O., and Quinlan, E.M. (2019). Homeostatic regulation of perisynaptic matrix metalloproteinase 9 (MMP9) activity in the amblyopic visual cortex. eLife *8*.

Niewmierzycka, A., Mills, J., St-Arnaud, R., Dedhar, S., and Reichardt, L.F. (2005). Integrin-linked kinase deletion from mouse cortex results in cortical lamination defects resembling cobblestone lissencephaly. The Journal of neuroscience : the official journal of the Society for Neuroscience *25*, 7022-7031.

Nishimoto, I., Okamoto, T., Matsuura, Y., Takahashi, S., Okamoto, T., Murayama, Y., and Ogata, E. (1993). Alzheimer amyloid protein precursor complexes with brain GTP-binding protein G(o). Nature *362*, 75-79.

Pagenstecher, A., Stalder, A.K., Kincaid, C.L., Shapiro, S.D., and Campbell, I.L. (1998). Differential expression of matrix metalloproteinase and tissue inhibitor of matrix metalloproteinase genes in the mouse central nervous system in normal and inflammatory states. Am J Pathol *152*, 729-741.

Palmeri, A., Ricciarelli, R., Gulisano, W., Rivera, D., Rebosio, C., Calcagno, E., Tropea, M.R., Conti, S., Das, U., Roy, S.*, et al.* (2017). Amyloid-beta Peptide Is Needed for cGMP-Induced Long-Term Potentiation and Memory. The Journal of neuroscience : the official journal of the Society for Neuroscience *37*, 6926-6937.

Parodi, J., Sepulveda, F.J., Roa, J., Opazo, C., Inestrosa, N.C., and Aguayo, L.G. (2010). Beta-amyloid causes depletion of synaptic vesicles leading to neurotransmission failure. The Journal of biological chemistry *285*, 2506-2514.

Patani, R., Hardingham, G.E., and Liddelow, S.A. (2023). Functional roles of reactive astrocytes in neuroinflammation and neurodegeneration. Nat Rev Neurol *19*, 395-409.

Plant, L.D., Boyle, J.P., Smith, I.F., Peers, C., and Pearson, H.A. (2003). The production of amyloid beta peptide is a critical requirement for the viability of central neurons. The Journal of neuroscience : the official journal of the Society for Neuroscience *23*, 5531-5535.

Puzzo, D., Privitera, L., Leznik, E., Fa, M., Staniszewski, A., Palmeri, A., and Arancio, O. (2008). Picomolar amyloid-beta positively modulates synaptic plasticity and memory in hippocampus. The Journal of neuroscience : the official journal of the Society for Neuroscience *28*, 14537-14545.

773 Qin, H., Yeh, W.I., De Sarno, P., Holdbrooks, A.T., Liu, Y., Muldowney, M.T., Reynolds, S.L., Yanagisawa,
774 L.L., Fox, T.H., 3rd, Park, K.*, et al.* (2012). Signal transducer and activator of transcription-3/suppressor of
775 cytokine signaling-3 (STAT3/SOCS3) axis in myeloid cells regulates neuroinflammation. Proceedings of
776 the National Academy of Sciences of the United States of America *109*, 5004-5009.

777 Ramaker, J.M., Swanson, T.L., and Copenhaver, P.F. (2013). Amyloid precursor proteins interact with the
778 heterotrimeric G protein Go in the control of neuronal migration. The Journal of neuroscience : the
779 official journal of the Society for Neuroscience *33*, 10165-10181.

780 Ramsden, M., Henderson, Z., and Pearson, H.A. (2002). Modulation of Ca2+ channel currents in primary
781 cultures of rat cortical neurones by amyloid beta protein (1-40) is dependent on solubility status. Brain
782 research *956*, 254-261.

783 Rice, H.C., Townsend, M., Bai, J., Suth, S., Cavanaugh, W., Selkoe, D.J., and Young-Pearse, T.L. (2012).
784 Pancortins interact with amyloid precursor protein and modulate cortical cell migration. Development
785 *139*, 3986-3996.

786 Satz, J.S., Ostendorf, A.P., Hou, S., Turner, A., Kusano, H., Lee, J.C., Turk, R., Nguyen, H., Ross-Barta, S.E.,
787 Westra, S.*, et al.* (2010). Distinct functions of glial and neuronal dystroglycan in the developing and adult
788 mouse brain. J Neurosci *30*, 14560-14572.

789 Sayed, F.A., Telpoukhovskaia, M., Kodama, L., Li, Y., Zhou, Y., Le, D., Hauduc, A., Ludwig, C., Gao, F.,
790 Clelland, C.*, et al.* (2018). Differential effects of partial and complete loss of TREM2 on microglial injury
791 response and tauopathy. Proceedings of the National Academy of Sciences of the United States of
792 America *115*, 10172-10177.

793 Schafer, D.P., and Stevens, B. (2015). Microglia Function in Central Nervous System Development and
794 Plasticity. Cold Spring Harb Perspect Biol *7*, a020545.

795 Shaked, G.M., Kummer, M.P., Lu, D.C., Galvan, V., Bredesen, D.E., and Koo, E.H. (2006). Abeta induces
796 cell death by direct interaction with its cognate extracellular domain on APP (APP 597-624). FASEB J *20*,
797 1254-1256.

798 Shankar, G.M., Li, S., Mehta, T.H., Garcia-Munoz, A., Shepardson, N.E., Smith, I., Brett, F.M., Farrell,
799 M.A., Rowan, M.J., Lemere, C.A.*, et al.* (2008). Amyloid-beta protein dimers isolated directly from
800 Alzheimer's brains impair synaptic plasticity and memory. Nat Med *14*, 837-842.

801 Shigemoto-Mogami, Y., Hoshikawa, K., Goldman, J.E., Sekino, Y., and Sato, K. (2014). Microglia enhance
802 neurogenesis and oligodendrogenesis in the early postnatal subventricular zone. The Journal of
803 neuroscience : the official journal of the Society for Neuroscience *34*, 2231-2243.

804 Spiller, K.J., Khan, T., Dominique, M.A., Restrepo, C.R., Cotton-Samuel, D., Levitan, M., Jafar-Nejad, P.,
805 Zhang, B., Soriano, A., Rigo, F.*, et al.* (2019). Reduction of matrix metalloproteinase 9 (MMP-9) protects
806 motor neurons from TDP-43-triggered death in rNLS8 mice. Neurobiol Dis *124*, 133-140.

807 Spolidoro, M., Putignano, E., Munafo, C., Maffei, L., and Pizzorusso, T. (2012). Inhibition of matrix
808 metalloproteinases prevents the potentiation of nondeprived-eye responses after monocular
809 deprivation in juvenile rats. Cereb Cortex *22*, 725-734.

810 Stellwagen, D., and Malenka, R.C. (2006). Synaptic scaling mediated by glial TNF-alpha. Nature *440*,
811 1054-1059.

812 Stenman, J., Toresson, H., and Campbell, K. (2003). Identification of two distinct progenitor populations
813 in the lateral ganglionic eminence: implications for striatal and olfactory bulb neurogenesis. The Journal
814 of neuroscience : the official journal of the Society for Neuroscience *23*, 167-174.

815 Stine, W.B., Jungbauer, L., Yu, C., and LaDu, M.J. (2011). Preparing synthetic Abeta in different
816 aggregation states. Methods Mol Biol *670*, 13-32.

817 Sturchio, A., Dwivedi, A.K., Malm, T., Wood, M.J.A., Cilia, R., Sharma, J.S., Hill, E.J., Schneider, L.S., Graff-
818 Radford, N.R., Mori, H.*, et al.* (2022). High Soluble Amyloid-beta42 Predicts Normal Cognition in
819 Amyloid-Positive Individuals with Alzheimer's Disease-Causing Mutations. J Alzheimers Dis.

820 Sturchio, A., Dwivedi, A.K., Young, C.B., Malm, T., Marsili, L., Sharma, J.S., Mahajan, A., Hill, E.J.,
821 Andaloussi, S.E., Poston, K.L.*, et al.* (2021). High cerebrospinal amyloid-beta 42 is associated with normal
822 cognition in individuals with brain amyloidosis. EClinicalMedicine *38*, 100988.

823 Tall, G.G., Krumins, A.M., and Gilman, A.G. (2003). Mammalian Ric-8A (synembryn) is a heterotrimeric
824 Galpha protein guanine nucleotide exchange factor. The Journal of biological chemistry *278*, 8356-8362.

825 Tan, J., Town, T., Paris, D., Mori, T., Suo, Z., Crawford, F., Mattson, M.P., Flavell, R.A., and Mullan, M.
826 (1999). Microglial activation resulting from CD40-CD40L interaction after beta-amyloid stimulation.
827 Science *286*, 2352-2355.

828 Tran, N.M., Shekhar, K., Whitney, I.E., Jacobi, A., Benhar, I., Hong, G., Yan, W., Adiconis, X., Arnold, M.E.,
829 Lee, J.M.*, et al.* (2019). Single-Cell Profiles of Retinal Ganglion Cells Differing in Resilience to Injury
830 Reveal Neuroprotective Genes. Neuron *104*, 1039-1055 e1012.

831 Tsiknia, A.A., Sundermann, E.E., Reas, E.T., Edland, S.D., Brewer, J.B., Galasko, D., Banks, S.J., and
832 Alzheimer's Disease Neuroimaging, I. (2022). Sex differences in Alzheimer's disease: plasma MMP-9 and
833 markers of disease severity. Alzheimers Res Ther *14*, 160.

834 Vainchtein, I.D., Chin, G., Cho, F.S., Kelley, K.W., Miller, J.G., Chien, E.C., Liddelow, S.A., Nguyen, P.T.,
835 Nakao-Inoue, H., Dorman, L.C.*, et al.* (2018). Astrocyte-derived interleukin-33 promotes microglial
836 synapse engulfment and neural circuit development. Science *359*, 1269-1273.

837 Walsh, D.M., Klyubin, I., Fadeeva, J.V., Cullen, W.K., Anwyl, R., Wolfe, M.S., Rowan, M.J., and Selkoe, D.J.
838 (2002). Naturally secreted oligomers of amyloid beta protein potently inhibit hippocampal long-term
839 potentiation in vivo. Nature *416*, 535-539.

840 Wang, H., Ng, K.H., Qian, H., Siderovski, D.P., Chia, W., and Yu, F. (2005). Ric-8 controls Drosophila neural
841 progenitor asymmetric division by regulating heterotrimeric G proteins. Nat Cell Biol *7*, 1091-1098.

842 Wang, X., Jung, J., Asahi, M., Chwang, W., Russo, L., Moskowitz, M.A., Dixon, C.E., Fini, M.E., and Lo, E.H.
843 (2000). Effects of matrix metalloproteinase-9 gene knock-out on morphological and motor outcomes
844 after traumatic brain injury. The Journal of neuroscience : the official journal of the Society for
845 Neuroscience *20*, 7037-7042.

846 Wang, Y., Fu, W.Y., Cheung, K., Hung, K.W., Chen, C., Geng, H., Yung, W.H., Qu, J.Y., Fu, A.K.Y., and Ip,
847 N.Y. (2021). Astrocyte-secreted IL-33 mediates homeostatic synaptic plasticity in the adult hippocampus.
848 Proceedings of the National Academy of Sciences of the United States of America *118*.

849 Yang, Y., Kim, J., Kim, H.Y., Ryoo, N., Lee, S., Kim, Y., Rhim, H., and Shin, Y.K. (2015). Amyloid-beta
850 Oligomers May Impair SNARE-Mediated Exocytosis by Direct Binding to Syntaxin 1a. Cell reports *12*,
851 1244-1251.

852 Yona, S., Kim, K.W., Wolf, Y., Mildner, A., Varol, D., Breker, M., Strauss-Ayali, D., Viukov, S., Guilliams, M.,
853 Misharin, A.*, et al.* (2013). Fate mapping reveals origins and dynamics of monocytes and tissue
854 macrophages under homeostasis. Immunity *38*, 79-91.

855 Yoshida, M., Assimacopoulos, S., Jones, K.R., and Grove, E.A. (2006). Massive loss of Cajal-Retzius cells
856 does not disrupt neocortical layer order. Development *133*, 537-545.

857 Young-Pearse, T.L., Bai, J., Chang, R., Zheng, J.B., LoTurco, J.J., and Selkoe, D.J. (2007). A critical function
858 for beta-amyloid precursor protein in neuronal migration revealed by in utero RNA interference. The
859 Journal of neuroscience : the official journal of the Society for Neuroscience *27*, 14459-14469.

860 Yu, D., Li, T., Delpech, J.C., Zhu, B., Kishore, P., Koshi, T., Luo, R., Pratt, K.J.B., Popova, G., Nowakowski,
861 T.J.*, et al.* (2022). Microglial GPR56 is the molecular target of maternal immune activation-induced
862 parvalbumin-positive interneuron deficits. Sci Adv *8*, eabm2545.

863 Zhang, Y., Chen, K., Sloan, S.A., Bennett, M.L., Scholze, A.R., O'Keeffe, S., Phatnani, H.P., Guarnieri, P.,
864 Caneda, C., Ruderisch, N.*, et al.* (2014). An RNA-sequencing transcriptome and splicing database of glia,
865 neurons, and vascular cells of the cerebral cortex. The Journal of neuroscience : the official journal of the
866 Society for Neuroscience *34*, 11929-11947.

867 Zhou, B., Lu, J.G., Siddu, A., Wernig, M., and Sudhof, T.C. (2022). Synaptogenic effect of APP-Swedish
868 mutation in familial Alzheimer's disease. Sci Transl Med *14*, eabn9380.

869 Zipp, F., Bittner, S., and Schafer, D.P. (2023). Cytokines as emerging regulators of central nervous system
870 synapses. Immunity *56*, 914-925.

871 Zott, B., Simon, M.M., Hong, W., Unger, F., Chen-Engerer, H.J., Frosch, M.P., Sakmann, B., Walsh, D.M.,
872 and Konnerth, A. (2019). A vicious cycle of beta amyloid-dependent neuronal hyperactivation. Science
873 *365*, 559-565.

874

875

878 ## Figures and legends

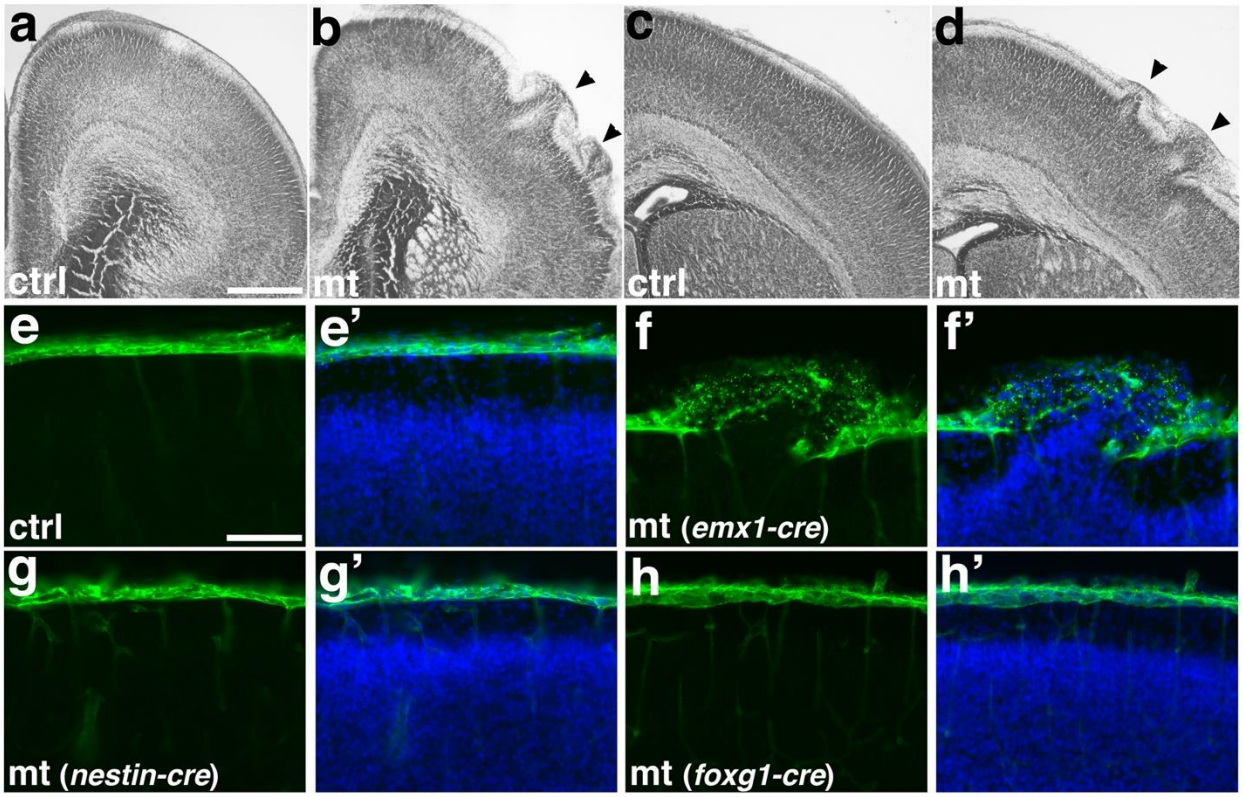

879

880 **Fig. 1. Deletion of *ric8a* using *emx1-cre* results in cortical ectopia due to non-neural deficits**.

881 (**a-d**) Nissl staining of control (ctrl, **a**&**c**) and mutant (mt, **b**&**d**) anterior motor (**a-b**) and posterior

882 somatosensory (**c-d**) cortex at P0.

883 **(e-e'**) Laminin (LN, in green) and nuclear (DAPI, in blue) staining of control cortices at P0. A continuous

884 basement membrane is observed at the pia, beneath which cells are well organized in the cortical wall.

885 (**f-f'**) Staining of *ric8a-emx1-cre* mutant cortices at P0. Basement membrane breach and neuronal

886 ectopia are observed following *ric8a* deletion by *emx1-cre*, a *cre* line expressed in cortical radial glial

887 progenitors beginning at E10.5.

888 **(g-g’**) Staining of *ric8a-nestin-cre* mutant cortices at P0. No obvious basement membrane breach or
889 neuronal ectopia is observed following *ric8a* deletion by *nestin-cre*, a *cre* line expressed in cortical
890 progenitors beginning around E12.5.

891 (**h-h’**) Staining of *ric8a-foxg1-cre* mutant cortices at P0. No obvious basement membrane breach or
892 neuronal ectopia is observed following *ric8a* deletion by *foxg1-cre*, a *cre* line expressed in forebrain
893 neural progenitors from E9.0.

894 Scale bars, 640μm for (**a-b**), 400μm for (**c-d**), and 100μm for (**e-h’**).
895
896

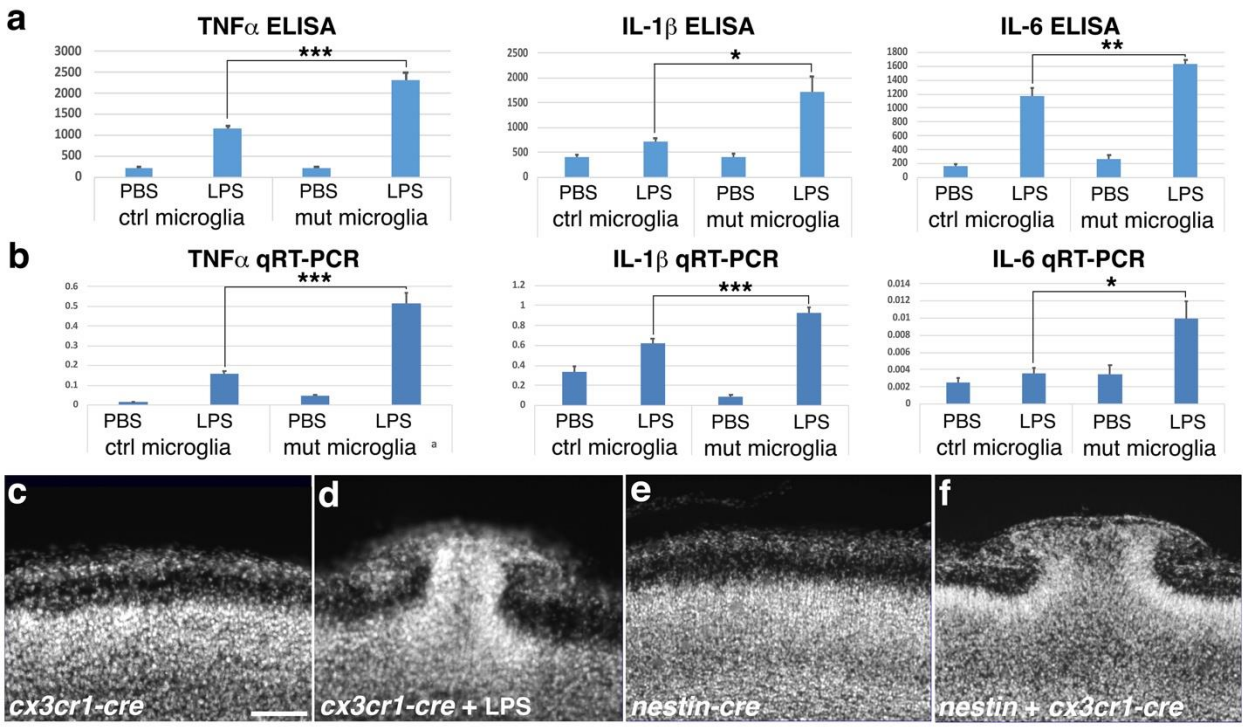

Fig. 2. *ric8a* deficiency in microglia is responsible for cortical ectopia.

(**a**) TNFα, IL-1β, and IL-6 secretion (pg/ml) in control and *ric8a/cx3cr1-cre* mutant microglia following LPS stimulation. *, $P < 0.05$; **, $P < 0.01$; ***, $P < 0.001$; n = 6-8 each group.

(**b**) TNFα, IL-1 β, and IL-6 mRNA expression in control and *ric8a/cx3cr1-cre* mutant microglia following LPS stimulation. *, $P < 0.05$; ***, $P < 0.001$; n = 5-6 each group.

(**c**-**d**) Nuclear (DAPI, in grey) staining of *ric8a-cx3cr1-cre* mutant cortices at P0 in the absence (**c**) or presence (**d**) of LPS treatment during embryogenesis.

(**e-f**) Nuclear (DAPI, in grey) staining of *ric8a-nestin-cre* single *cre* (**e**) and *ric8a-nestin-cre+cx3cr1-cre* double *cre* (**f**) mutant cortices at P0.

Scale bar in (**c**), 100 μm for (**c-f**).

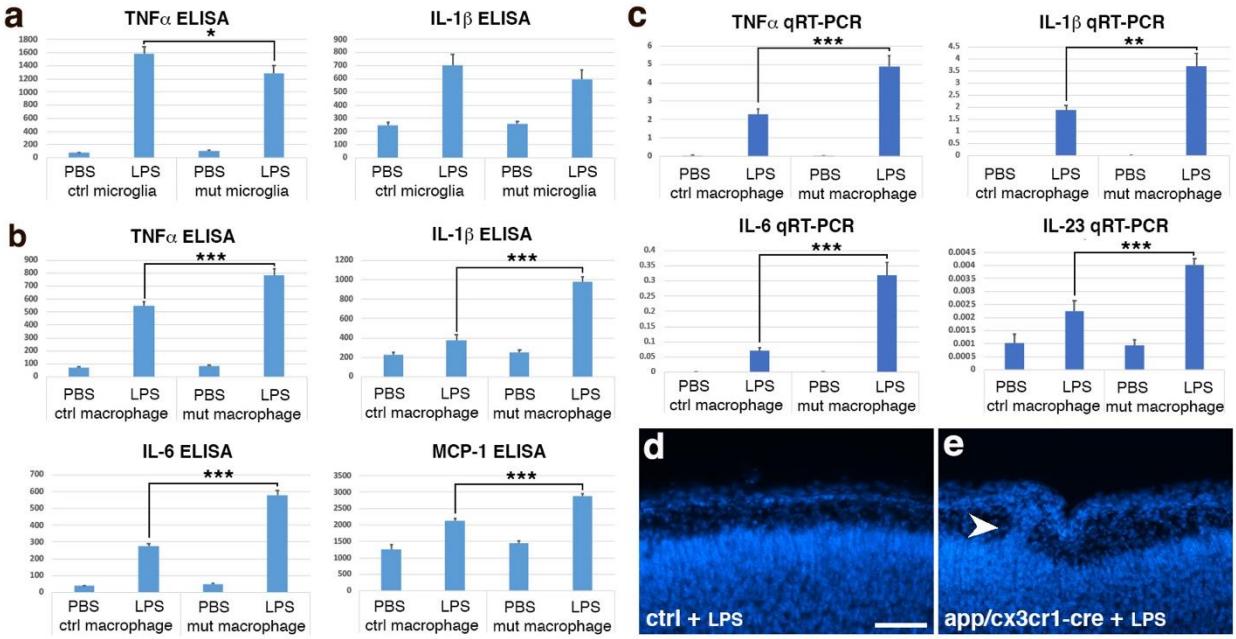

Fig. 3. *app* deficiency results in hypersensitive microglia and cortical ectopia.

(a) TNFα and IL-1β secretion (pg/ml) in cultured control and *app/cx3cr1-cre* mutant microglia following LPS stimulation. *, $P < 0.05$; n = 7-9 each group.

(**b**) TNFα, IL-1β, IL-6, and MCP1 secretion (pg/ml) in fresh unelicited control and *app/cx3cr1-cre* mutant peritoneal macrophages following LPS stimulation. ***, $P < 0.001$; n = 7-10 each group.

(**c**) TNFα, IL-1 β, IL-6, and IL-23 mRNA expression in fresh unelicited control and *app/cx3cr1-cre* mutant peritoneal macrophages following LPS stimulation. **, $P < 0.01$; ***, $P < 0.001$; n = 6 each group

(**d-e**) Nuclear (DAPI, in blue) staining of control (**D**) and LPS-treated *app/cx3cr1-cre* mutant (**E**) cortices at P0. Note cortical ectopia in the mutant cortex (arrowhead).

Scale bar in (**d**), 200μm for (**d-e**).

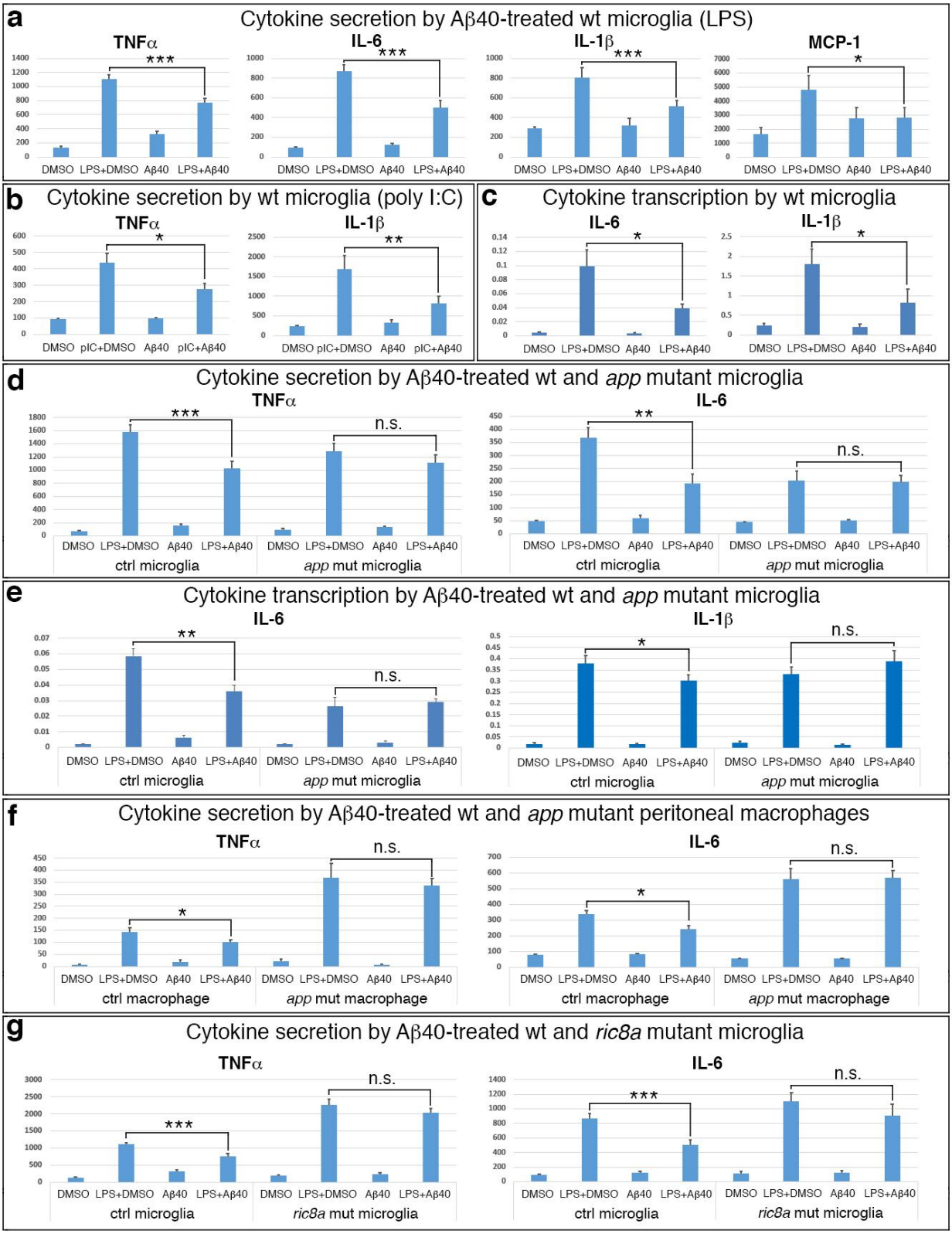

Fig. 4. Monomeric Aβ40 suppresses microglia via an APP and Ric8a.

924 **(a**) TNFα, IL-6, IL-1β, and MCP1 secretion (pg/ml) by wildtype microglia following LPS stimulation in the

925 absence or presence of Aβ40 (200 or 500nM). *, $P < 0.05$; ***, $P < 0.001$; n = 8-14 each group.

926 **(b**) TNFα and IL-1β secretion (pg/ml) by wildtype microglia following poly I:C stimulation in the absence

927 or presence of Aβ40 (500nM). *, $P < 0.05$; **, $P < 0.01$; n = 6-7 each group.

928 **(c**) IL-6 and IL-1β mRNA induction in wildtype microglia following LPS stimulation in the absence or

929 presence of Aβ40 (500nM). *, $P < 0.05$; n = 6 each group.

930 **(d**) TNFα and IL-6 secretion (pg/ml) by control and *app/cx3cr1-cre* mutant microglia following LPS

931 stimulation in the absence or presence of Aβ40 (200nM). **, $P < 0.01$; ***, $P < 0.001$; n = 8 each group.

932 **(e**) IL-6 and IL-1β mRNA induction in control and *app/cx3cr1-cre* mutant microglia following LPS

933 stimulation in the absence or presence of Aβ40 (200nM). *, $P < 0.05$; **, $P < 0.01$; n = 6 each group.

934 **(f**) TNFα and IL-6 secretion (pg/ml) by control and *app/cx3cr1-cre* mutant peritoneal macrophages

935 following LPS stimulation in the absence or presence of Aβ40 (500nM). *, $P < 0.05$; n = 6-7 each group

936 **(g**) TNFα and IL-6 secretion (pg/ml) by control and *ric8a/cx3cr1-cre* mutant microglia following LPS

937 stimulation in the absence or presence of Aβ40 (200nM). ***, $P < 0.001$; n = 12-14 each group.

938

939

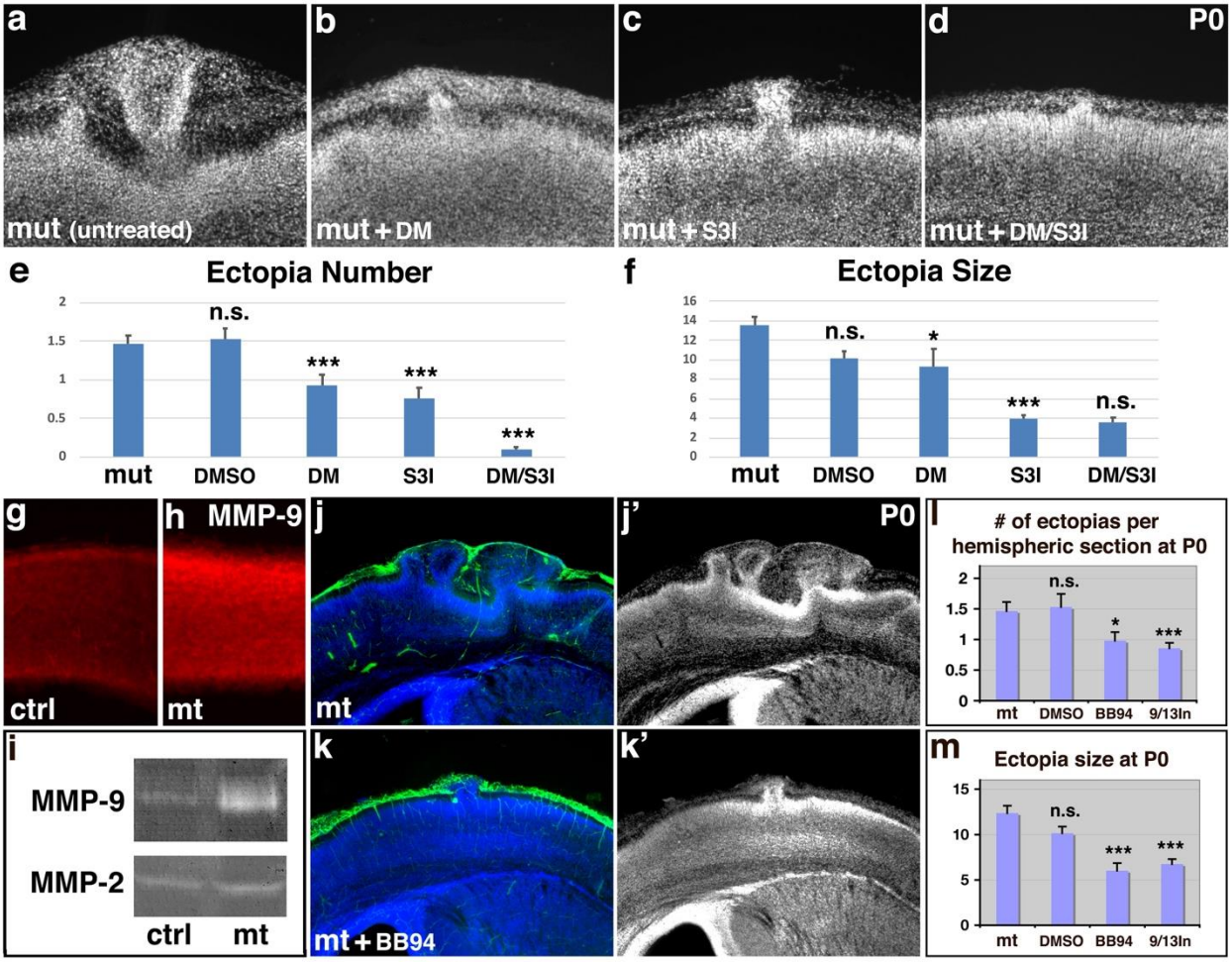

Fig. 5. Inhibition of both microglial inflammatory activation and cortical MMP9 activity suppresses basement membrane breach and neuronal ectopia.

(**a-d**) Nuclear (DAPI, in grey) staining of untreated (**a**), anti-inflammatory drug dorsomorphin (DM) (**b**), Stat3 inhibitor S3I-201 (S3I) (**c**), and DM/S3I (**d**) dual treated mutant cortices at P0.

(**e-f**) Quantitative analysis of ectopia number (**e**) and size (**f**) in the neonatal mutant cortex after DMSO, DM, S3I, and DM/S3I dual treatment at E12.5. *, $P < 0.05$; ***, $P < 0.001$; all compared to untreated mutants. The reduction in ectopia size after dual treatment is not statistically significant, likely due to the small number of ectopias that remained.

949 (**g**-**h**) MMP9 (in red) staining of control (**g**) and mutant cortices (**h**) at E13.5. Quantification shows

950 statistically significant increases in mutants (control, 24.8 ± 0.2 AU (Arbitrary Units); mutant, 35.7 ± 1.7

951 AU; $P = 0.002$; n = 6).

952 (**i**) Gel zymography of control and mutant cortical lysates at E13.5. Increased levels of MMP9 but not of

953 MMP2 were observed in mutants (control, 1.00 ± 0.06 AU; mutant, 3.72 ±1.86 AU; $P = 0.028$; n = 4)

954 (**j-k'**) Laminin (in green) and nuclear (DAPI, in blue) staining of mutant cortices untreated (**H**) or treated

955 (**I**) with BB94.

956 (**l-m**) Quantitative analysis of ectopia number and size following MMP inhibitor BB94 or MMP9/13

957 inhibitor treatment. *, $P < 0.05$; ***, $P < 0.001$; all compared to untreated mutants.

958

959

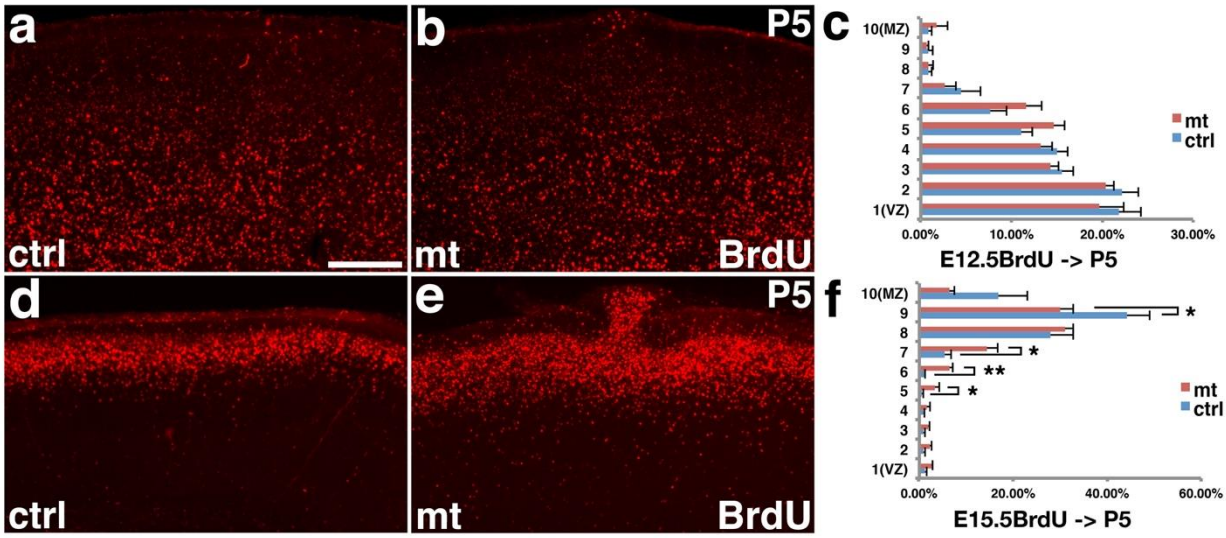

Supplemental Fig. 1. Birth-dating of early and late-born neurons in *ric8a-emx1-cre* mutant cortices. (**a-c**) BrdU (in red) staining in control (**a**) and mutant (**b**) cortices at P5 after administration at E12.5. Quantification is shown in (**c**). No statistically significant differences were observed between control and mutant neurons in regions without ectopia.

(**d-f**) BrdU staining in control (**d**) and mutant (**e**) cortices at P5 after administration at E15.5. Quantification is shown in (**f**). Neuronal migration appears slightly delayed in mutants as compared to controls. *, $P < 0.05$; **, $P < 0.01$; n = 5.

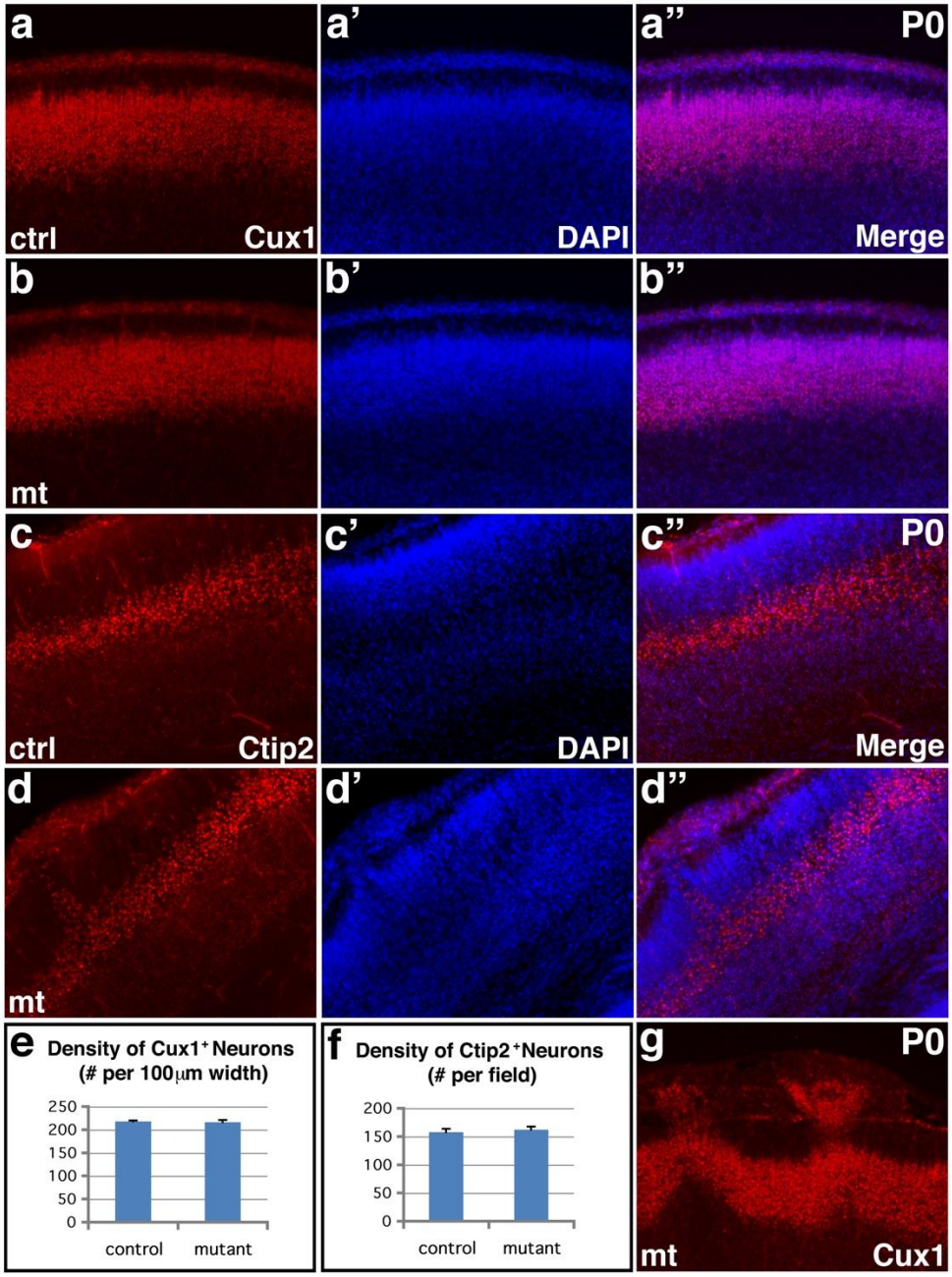

Supplemental Fig. 2. Lamina-specific neuronal markers are normal outside ectopia in *ric8a-emx1-cre* mutant cortices.

(**a**-**b**") Cux1 (in red) and nuclear (DAPI, in blue) staining of control (**a-a"**) and mutant (**b-b"**) cortices at P0 in a region without ectopia. No obvious changes in the expression pattern of Cux1, an upper layer neuronal marker, were observed in the mutant cortex, except in areas with ectopia (see panel (**g**)).

975 (**c**-**d**”) Ctip2 (in red) and nuclear (DAPI, in blue) staining of control (**c**-**c**”) and mutant (**d**-**d**”) cortices at P0.

976 No obvious changes in the expression pattern of Ctip2, a deep layer neuronal marker, were observed in

977 the mutant cortex, except in areas with ectopia.

978 (**e**-**f**) Quantification of cortical neurons positive for Cux1 (**e**) and Ctip2 (**f**) in matching cortical regions at

979 P0. No significant differences were observed in the density of Cux1 (control, 218.1 $\pm$ 1.7 per 100 μm

980 cortical width; mutant, 216.4 $\pm$ 4.3 per 100 μm cortical width; P = 0.36, n = 12) or Ctip2 (control, 157.8 $\pm$

981 5.0 per field; mutant, 161.9 $\pm$ 5.9 per field; P = 0.31, n = 12) positive neurons between controls and

982 mutants.

983 (**g**) Cux1 (in red) staining of mutant cortices at P0 in a region with ectopia.

984 Scale bar in (**a**), 200 μm for all panels.

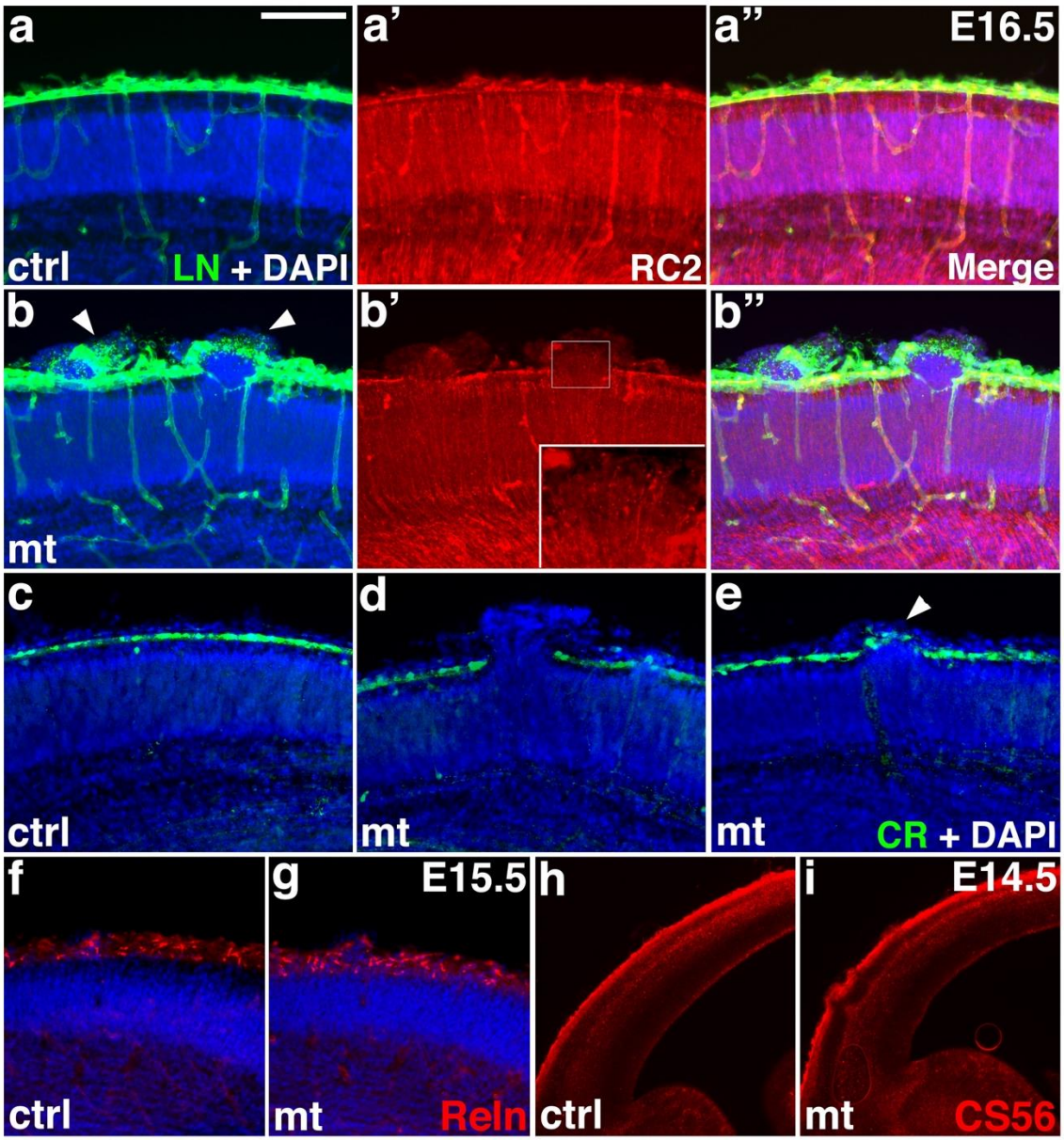

Supplemental Fig. 3. Neuronal ectopia in *ric8a-emx1-cre* mutants result from pial basement membrane breach during embryogenesis.

(a-a") Laminin (LN, in green), radial glial marker RC2 (in red), and nuclear (DAPI, in blue) staining of control cortices at E16.5. A continuous basement membrane is observed at the pia, where radial glial endfeet are anchored.

991 (**b**-**b”**) Laminin, RC2, and nuclear staining of *ric8a/emx1-cre* mutant cortices at E16.5. Neuronal ectopias
992 are consistently observed at sites of basement membrane breakage (arrowheads in **b**). Radial glial fibers
993 at these sites extend beyond the pia (inset in **b’**).

994 (**c**-**e**) Calretinin (CR, in green) and nuclear (DAPI, in blue) staining of control (**c**) and mutant (**d-e**) cortices
995 at E16.5. A continuous row of Calretinin positive Cajal-Retzius cells is observed in the marginal zone of
996 control cortices (**c**). By contrast, in mutants, Cajal-Retzius cells are absent at large ectopias (**d**). However,
997 they appear passively displaced by over-migrating neurons at small ectopias (arrowhead in **e**).

998 **(f-g**) Reelin (Reln, in red) and nuclear (DAPI, in blue) staining of control (**f**) and *ric8a*/*emx1-cre* mutant (**g**)
999 cortices at E15.5. Strong Reelin expression is observed in Cajal-Retzius cells in the marginal zone of both
1000 control and mutant cortices.

1001 **(h-i)** Chondroitin sulfate proteoglycan (CS56, in red) staining of control (**h**) and mutant (**i**) cortices at
1002 E14.5. Normal preplate splitting is observed in mutants.

1003 Scale bar in (**a**), 200μm for (**a**-**g)** and 500μm for (**h**-**i**).

1004

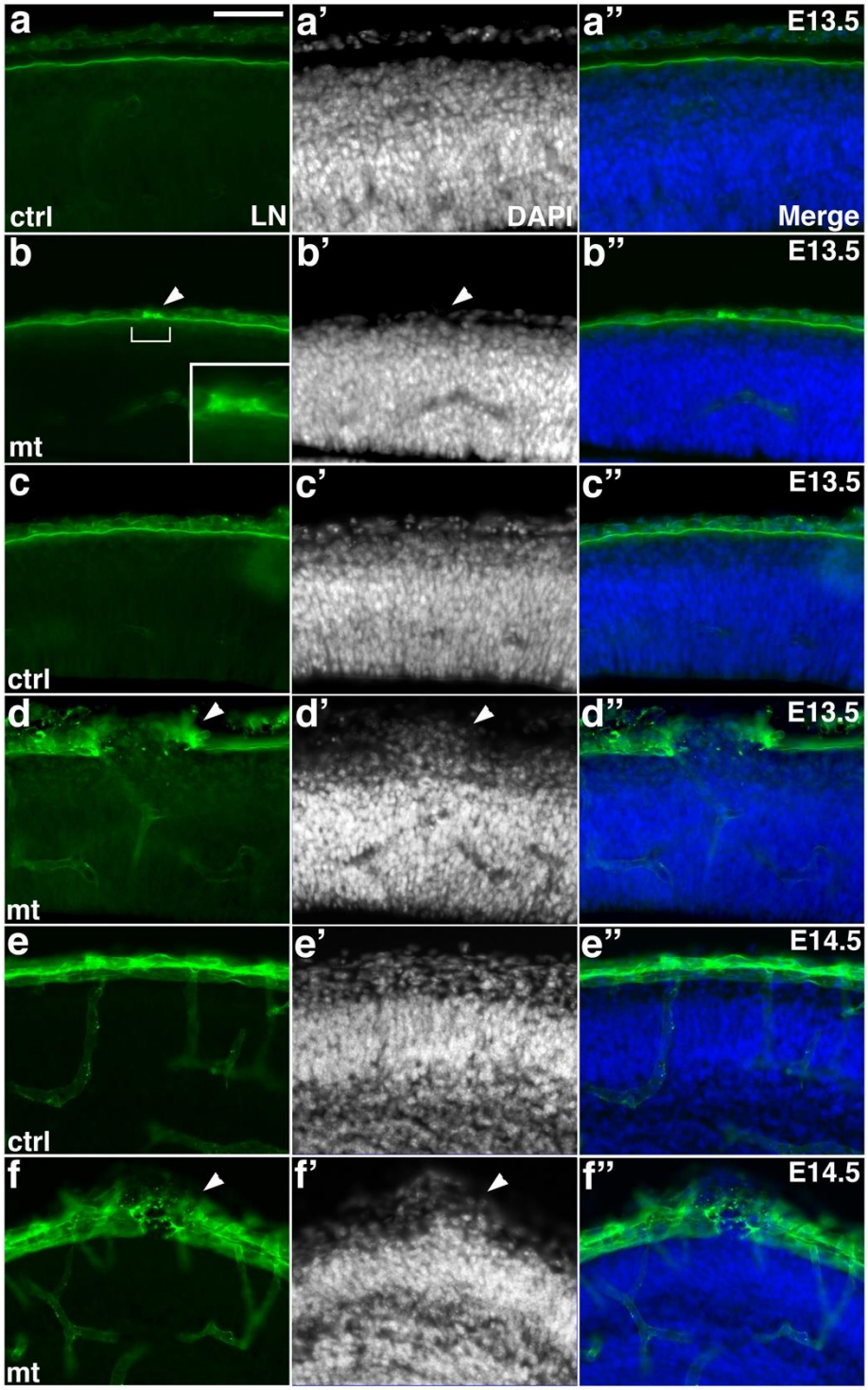

1005

1006 **Supplemental Fig. 4. Basement membrane breaches precede neuronal ectopia in *ric8a-emx1-cre* mutant**

1007 **cortices.**

1008 **(a**-**a”**) Laminin (LN, in green) and nuclear (DAPI, in blue) staining of control cortices at E13.5. A
1009 continuous basement membrane is observed at the pia, beneath which cells are well organized in the
1010 cortical wall.

1011 (**b**-**b”**) Laminin and nuclear staining of *ric8a-emx1-cre* mutant cortices at E13.5. In a subset of mutants, a
1012 small disruption of basement membrane is observed (bracket and inset in **b**), but not yet associated with
1013 ectopia (arrowhead in **b’**).

1014 **(c**-**c”**) Laminin (LN, in green) and nuclear (DAPI, in blue) staining of control cortices at E13.5.

1015 (**d**-**d”**) Laminin and nuclear staining of *ric8a-emx1-cre* mutant cortices at E13.5. Although at E13.5 we
1016 observe basement membrane defects in the absence of neuronal ectopia (see **b-b”**), when there are
1017 neuronal ectopia, they are always associated with basement membrane breakage.

1018 (**e**-**e”**) Laminin and nuclear staining of control cortices at E14.5.

1019 (**f**-**f”**) Laminin and nuclear staining of *ric-8a-emx1-cre* mutant cortices at E14.5. Neuronal ectopia at
1020 E14.5 are also always associated with basement membrane breakage.

1021 Scale bar in (**a**), 100 μm for all panels.

1022

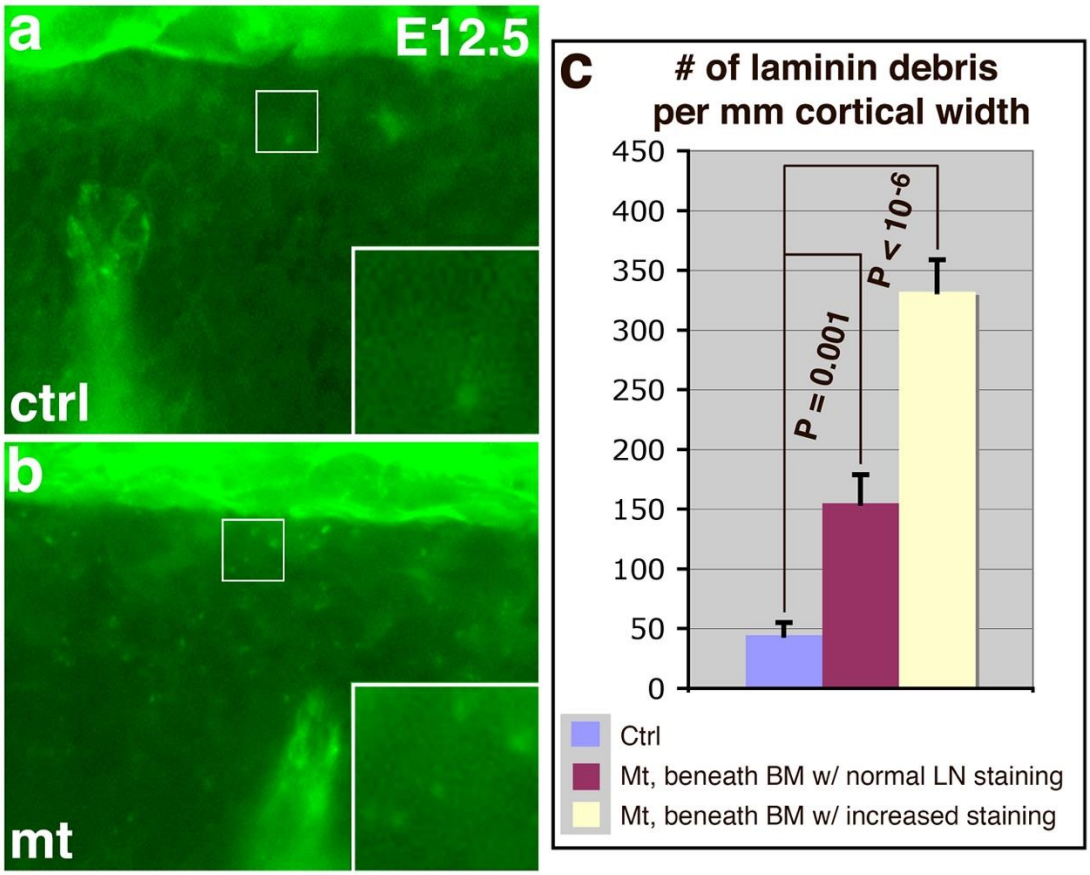

Supplemental Fig. 5. Signs of basement membrane degradation before breach formation at E12.5. (**a-b**) Laminin (in green) staining of control (**a**) and *ric8a-emx1-cre* mutant (**b**) cortices at E12.5. Increased numbers of laminin positive debris were observed in mutants (compare insets), even though breaches had yet to form.

(**c**) Quantitative analysis shows significant increases.

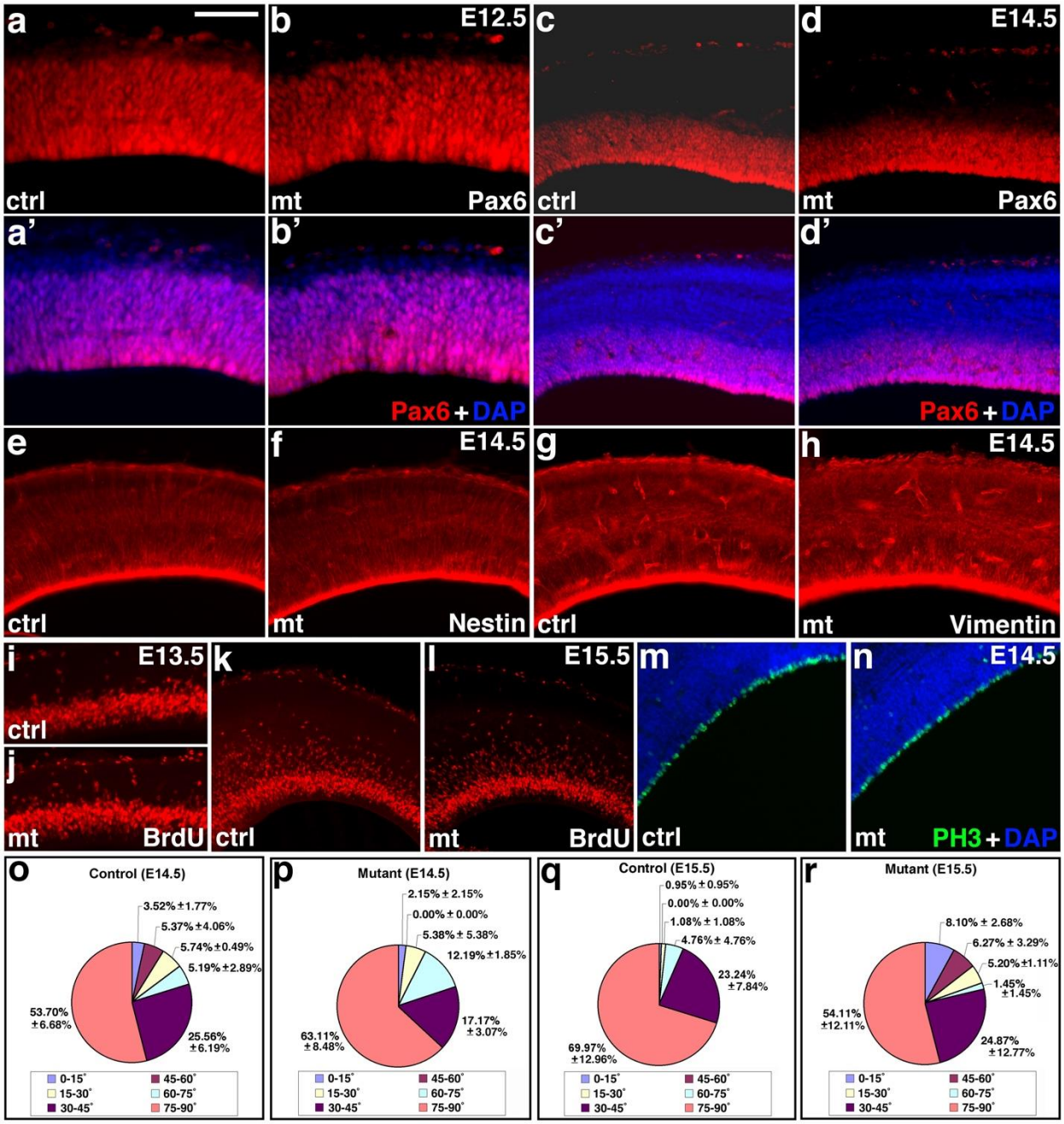

Supplemental Fig. 6. Cortical radial glial identity and proliferation are unaffected in *ric8a-emx1-cre* mutants.

(**a**-**b'**) Pax6 (in red) and nuclear (DAPI, in blue) staining of control (**a**&**a'**) and mutant (**b**&**b'**) cortices at E12.5.

1035 (**c**-**d'**) Pax6 (in red) and nuclear (DAPI, in blue) staining of control (**c**&**c'**) and mutant (**d**&**d'**) cortices at

1036 E14.5. No ectopic Pax6 positive cells were observed at either E12.5 or E14.5.

1037 **(e-f**) Nestin (in red) and nuclear (DAPI, in blue) staining of control (**e**) and mutant (**f**) cortices at E14.5.

1038 (**g**-**h**) Vimentin (in red) and nuclear (DAPI, in blue) staining of control (**g**) and mutant (**h**) cortices at E14.5.

1039 **(i-j**) BrdU staining (in red) in control (**i**) and mutant (**j**) cortices at E13.5.

1040 (**k-l**) BrdU staining (in red) in control (**k**) and mutant (**l**) cortices at E15.5.

1041 (**m-n**) Phospho-histone 3 (PH3, in green) and nuclear (DAPI, in blue) staining of control (**m**) and mutant

1042 (**n**) cortices at E14.5.

1043 **(o-p**) Cleavage plane distribution of radial glial mitosis in control (**o**) and mutant (**p**) cortices at E14.5. No

1044 significant differences were observed ($P > 0.4$, n = 3 animals each genotype; 73 cells for controls and 76

1045 cells for mutants).

1046 (**q**-**r**) Cleavage plane distribution of radial glial mitosis in control (**q**) and mutant (**r**) cortices at E15.5. No

1047 significant differences were observed ($P > 0.1$, n = 3 animals each genotype; 70 cells for controls and 59

1048 cells for mutants).

1049 Scale bar in (**a**), 100 μm for (**a**-**b'**) and 200 μm for (**c-n**).

1050

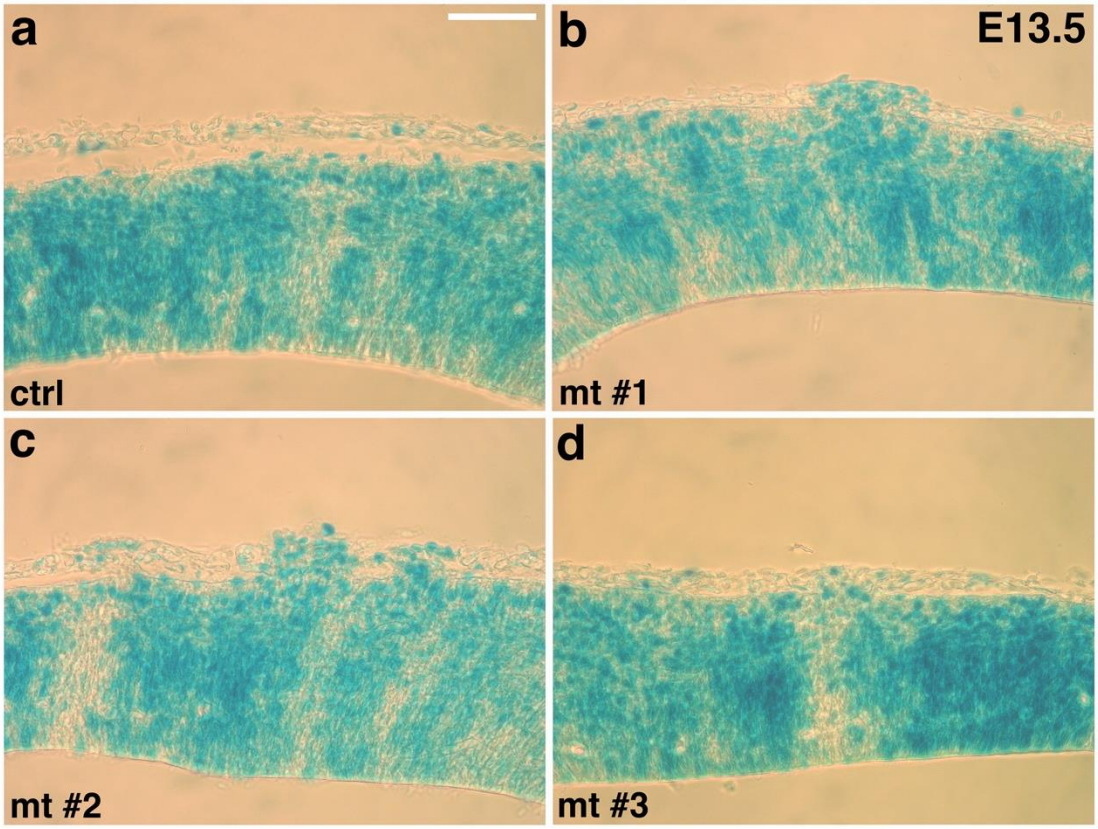

1051

1052 **Supplemental Fig. 7. Wnt pathway activity is normal in *ric8a-emx1-cre* mutant cortices.**

1053 X-gal staining of BAT-lacZ expression in *ric8a-emx1-cre* control (**a**) and mutant (**b**-**d**) cortices at E13.5. No

1054 obvious differences are observed between controls and three different mutants at this stage.

1055

1056

1057

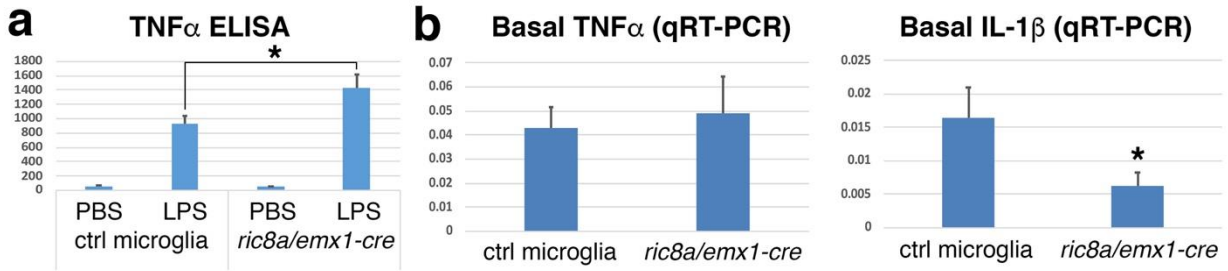

1058

1059 **Supplemental Fig. 8. *emx1-cre* is active in microglia.**

1060 TNFα secretion (pg/ml) (**a**) and basal TNFα and IL-1β mRNA expression (**b**) in control and *ric8a-emx1-cre*

1061 mutant microglia. *, $P < 0.05$; n = 5-8 each group.

1062

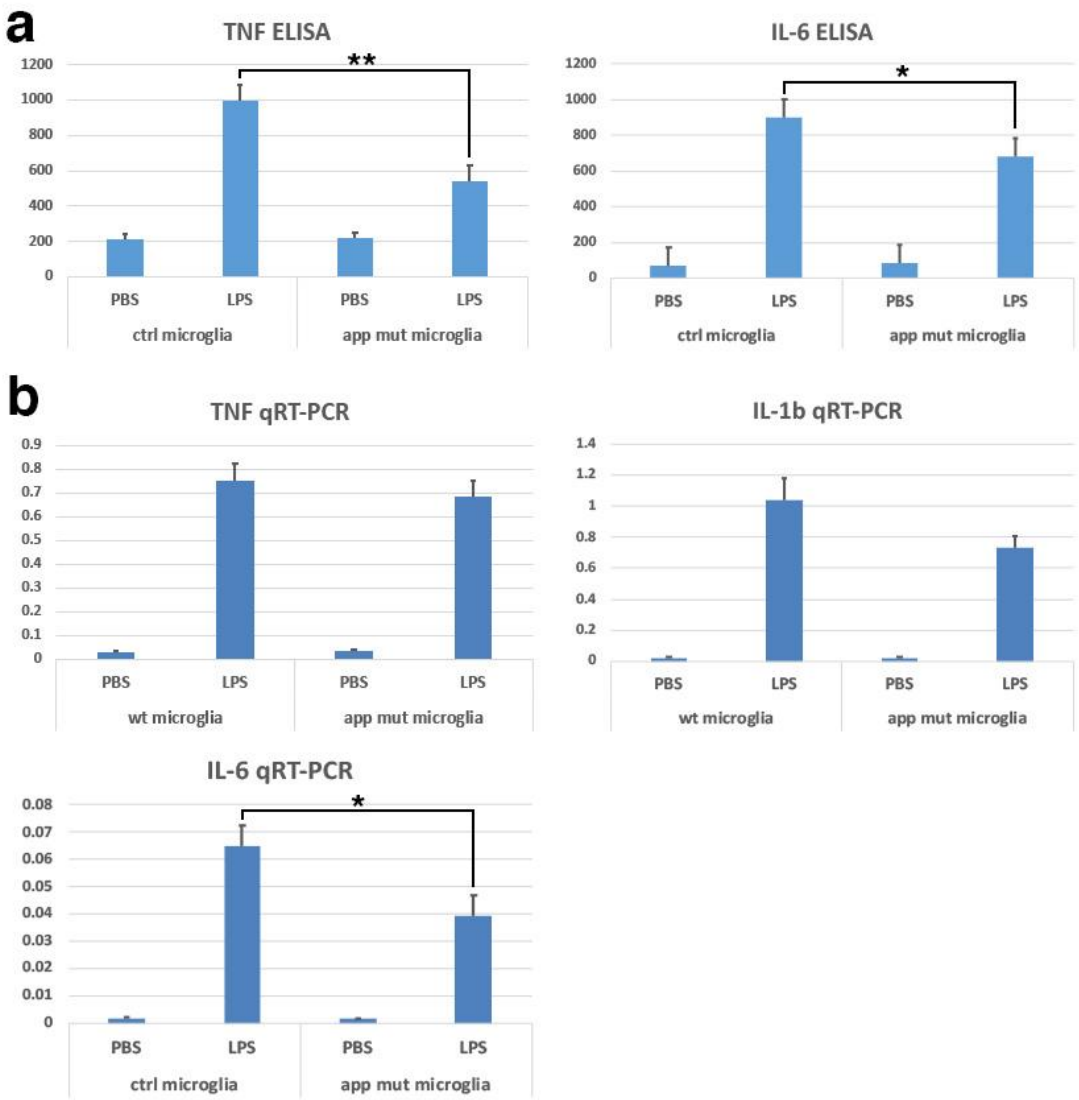

Supplemental Fig. 9. Cytokine secretion and transcriptional induction in *app-cx3cr1-cre* mutant microglia.

(a) TNFα and IL-6 secretion (pg/ml) in control and *app-cx3cr1-cre* mutant microglia following overnight LPS stimulation. *, $P < 0.05$; **, $P < 0.01$; n = 9-13 each group.

(**b**) TNFα, IL-1β and IL-6 mRNA expression in control and *app-cx3cr1-cre* mutant microglia following overnight 3-hr LPS stimulation. *, $P < 0.05$; n = 6-7 each group.

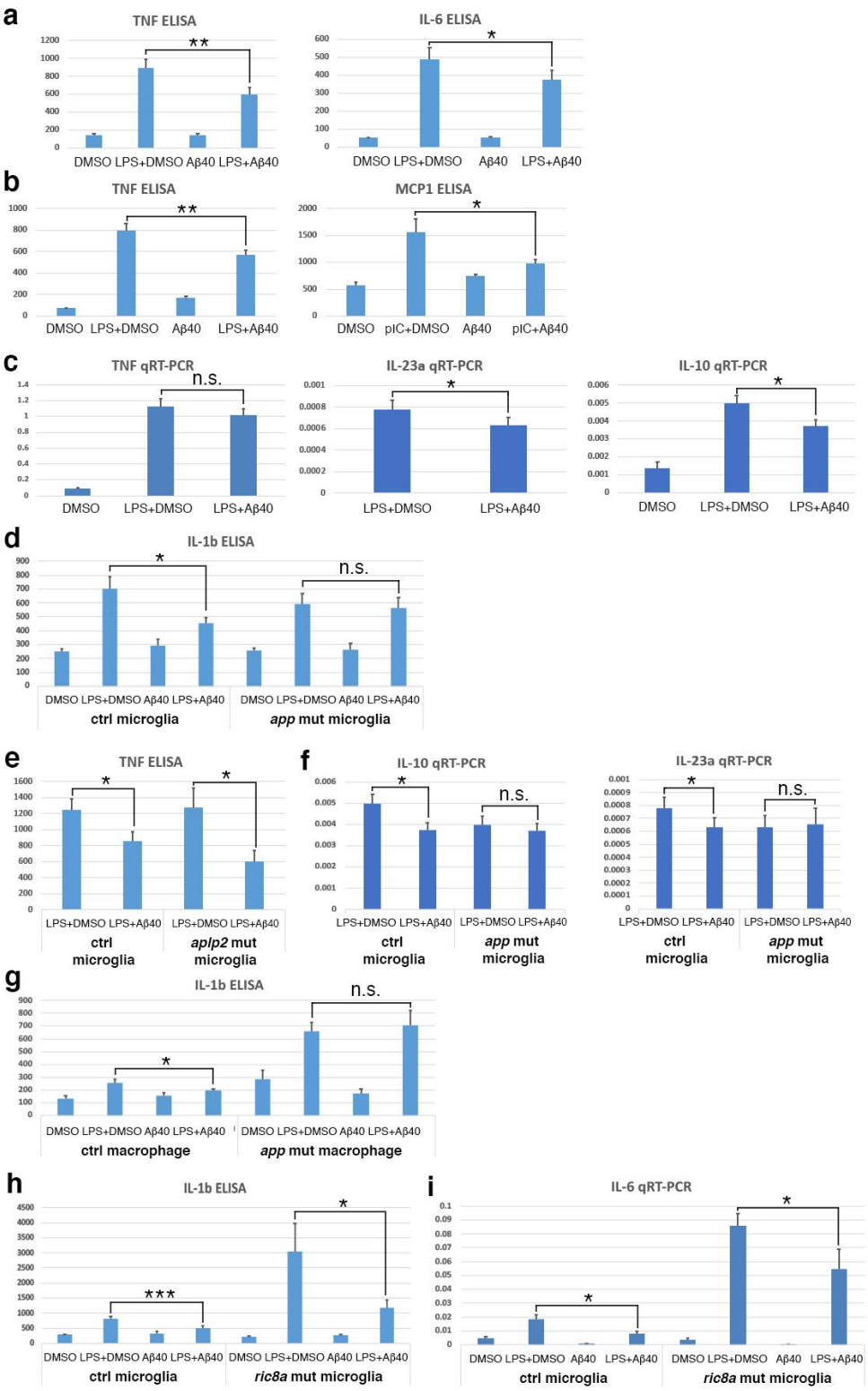

1071

1072 **Supplemental Fig. 10. Effects of monomeric Aβ on cytokine secretion and transcription in control and**

1073 **mutant microglial lineage cells.**

1074 **(a)** TNFα and IL-6 secretion (pg/ml) in wildtype microglia following LPS stimulation in the absence or
1075 presence of Aβ40 (50nM). *, $P < 0.05$; **, $P < 0.01$; n = 25 each group for TNFα and 11 each group for IL-
1076 6.

1077 (**b**) TNFα and MCP1 secretion (pg/ml) in wildtype microglia following LPS stimulation in the absence or
1078 presence of Aβ40 (500nM) from Genscript. Effects on IL-1β secretion in **Fig. 4b** was also performed with
1079 Genscript Aβ40. All other experiments in Fig. 7 were performed with ApexBio Aβ40. *, $P < 0.05$; **, $P <$
1080 0.01; n = 5-7 each group.

1081 (**c**) TNFα, IL-23, and IL-10 mRNA expression in wildtype microglia following LPS stimulation in the
1082 absence or presence of Aβ40 (400nM). *, $P < 0.05$; n = 6 each group

1083 **(d)** IL-1β secretion (pg/ml) in control and *app/cx3cr1-cre* mutant microglia following LPS stimulation in
1084 the absence or presence of Aβ40. *, $P < 0.05$; n = 8-12 each group.

1085 **(e)** TNFα (pg/ml) in control or *aplp2/cx3cr1-cre* mutant microglia following LPS stimulation in the
1086 absence or presence of Aβ40 (400nM). *, $P < 0.05$; n = 9-13 each group.

1087 **(f)** IL-10 and IL-23 mRNA expression in control and *app/cx3cr1-cre* mutant microglia following LPS
1088 stimulation in the absence or presence of Aβ40 (400nM). *, $P < 0.05$; n = 6 each group.

1089 **(g)** IL-1β secretion (pg/ml) in fresh unelicited control and *app/cx3cr1-cre* mutant peritoneal
1090 macrophages following LPS stimulation in the absence or presence of Aβ40 (400nM). *, $P < 0.05$; n = 12
1091 each group.

1092 (**h**) IL-1β secretion (pg/ml) in f control and *ric8a/cx3cr1-cre* mutant microglia following LPS stimulation in
1093 the absence or presence of Aβ40 (500nM). *, $P < 0.05$; ***, $P < 0.001$; n = 7-8 each group.

1094 (**i**) IL-6 mRNA expression in control and *ric8a/cx3cr1-cre* mutant microglia following LPS stimulation in

1095 the absence or presence of Aβ40 (200nM). *, $P < 0.05$; n = 6 each group.

1096

1097

1098

1099

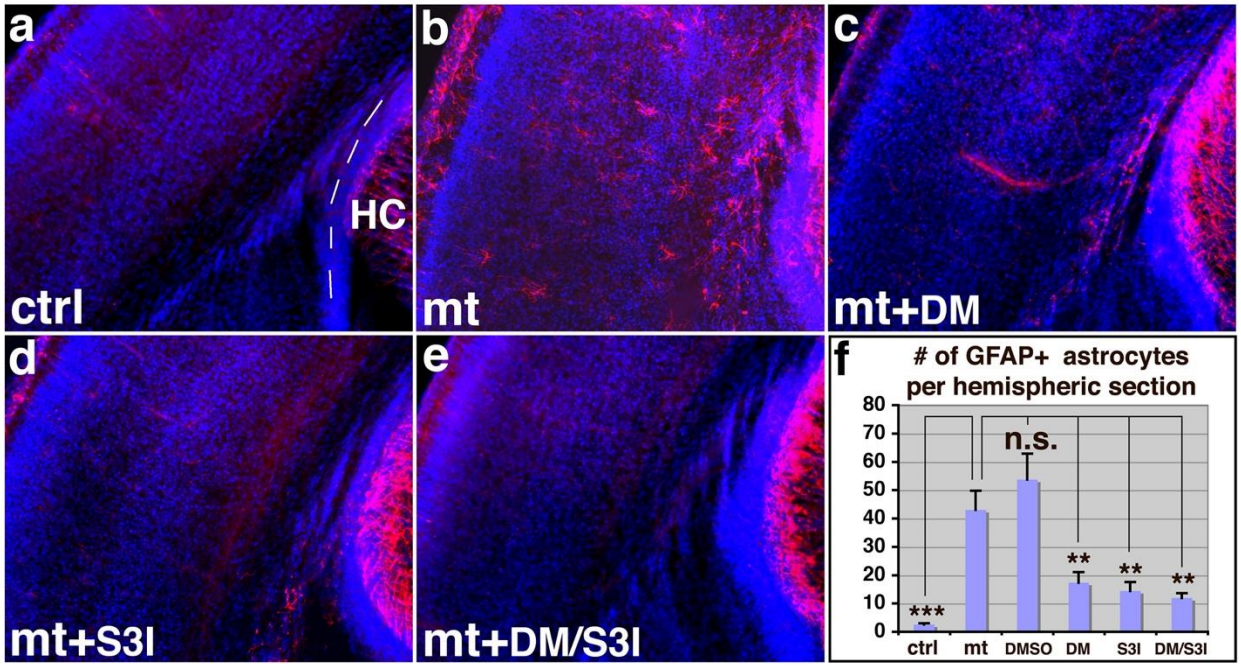

Supplemental Fig. 11. Suppression of astrogliosis in *ric8a-emx1-cre* mutant cortices by anti-inflammatory drugs, dorsomorphin (DM) and S3I-201 (S3I).

(a-e) GFAP (in red) and nuclear (DAPI, in blue) staining of neonatal control (**E**) and mutant cortices without treatment (**F**) or mutant cortices after dorsomorphin (DM, **G**), S3I-201 (S3I, **H**), or dual (DM+S3I, **I**) treatment at E12.5. Note, GFAP is normally expressed in the neonatal hippocampus (HC) (dashed line in (a)).

(f) Quantitative analysis of GFAP-positive astrocyte numbers in the neonatal mutant cortex after treatment at E12.5.

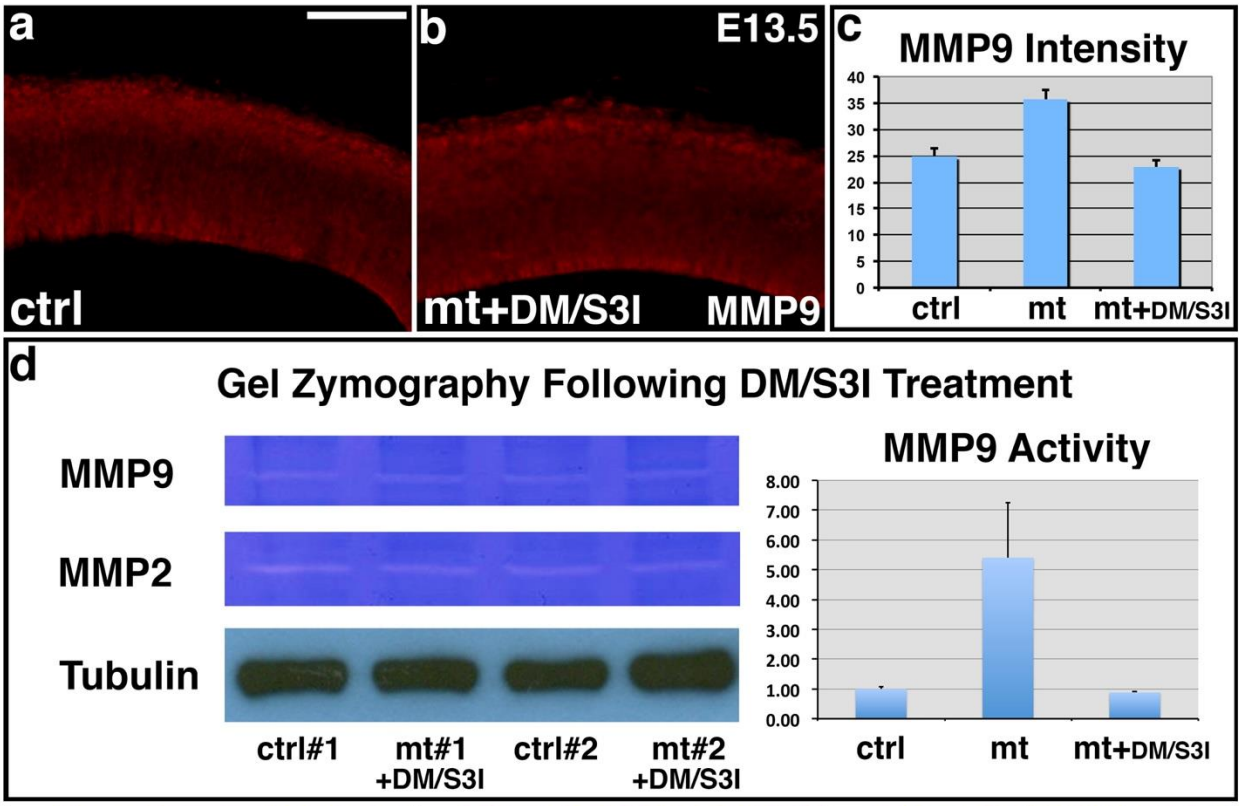

Supplemental Fig. 12. Suppression of MMP9 expression in *ric8a-emx1-cre* mutant cortices by anti-inflammatory drugs, dorsomorphin (DM) and S3I-201 (S3I).

(**a**) MMP9 (in red) staining in control cortices at E13.5.

(**b**) MMP9 (in red) staining in mutant cortices at E13.5 after DM and S3I dual treatment at E12.5.

(**c**) Quantitative analysis of MMP9 expression. No significant differences are observed in mutants after inhibitor treatment in comparison to controls (P = 0.44, n = 6).

(**d**) Gel zymography of E13.5 control and mutant cortical lysates following DM/S3I treatment at E12.5. Similar levels of MMP9 are observed between controls and mutants. Quantification also showed no significant differences in normalized MMP9 levels (P = 0.46, n = 4).

1125